

# **Synthesis and Characterization of Alginate/Poly (4-vinylpyridine) Hybrid System**

**Abdallah M. H. Alshhab**

Submitted to the  
Institute of Graduate Studies and Research  
in partial fulfillment of the requirements for the degree of

Doctor of Philosophy  
in  
Chemistry

Eastern Mediterranean University  
January 2020  
Gazimağusa, North Cyprus

Approval of the Institute of Graduate Studies and Research

---

Prof. Dr. Ali Hakan Ulusoy  
Director

I certify that this thesis satisfies all the requirements as a thesis for the degree of Doctor of Philosophy in Chemistry.

---

Prof. Dr. İzzet Sakallı  
Chair, Department of Chemistry

We certify that we have read this thesis and that in our opinion it is fully adequate in scope and quality as a thesis for the degree of Doctor of Philosophy in Chemistry.

---

Prof. Dr. Elvan Yılmaz  
Supervisor

---

Examining Committee

1. Prof. Dr. Gülsen Asman
2. Prof. Dr. Mustafa Gazi
3. Prof. Dr. Şadi Şen
4. Prof. Dr. Elvan Yılmaz
5. Assoc. Prof. Dr. Terin Adalı

---

---

---

---

---

## ABSTRACT

Polyelectrolyte multilayer (PEC) films of sodium alginate and poly(4-vinylpyridine) were prepared by immersing the sodium alginate (Na-Alg) films into the poly(4vinylpyridine) (P<sub>4</sub>VP) in 0.1 M hydrochloric acid solution. Then, the multilayer films were formed by the alternating addition of Na-Alg and P<sub>4</sub>VP respectively. The morphology, topography and chemical structures of the PEC films and its precursors were investigated and characterized by SEM analysis, AFM and FTIR spectroscopy respectively. It was observed that the number of layers and the nature of the outer layer affect the physicochemical characteristics. The thermal properties of the PEC films were examined by thermogravimetric analysis (TGA). The onset of degradation for PEC-2, PEC-3, PEC-4 and PEC-5 is at 180°C, 195°C, 195°C and 200°C respectively. Na-Alg film, on the other hand, decomposes at 215°C while P<sub>4</sub>VP film gives its first decomposition temperature at 290°C. The crystallinity indexes were calculated by XRD analysis. Complexation reduces the crystallinity comparing with the parent membrane, Na-Alg. Crystallinity index of Na-Alg film is 0.49 whereas the values for PEC-2, PEC-3, PEC-4 and PEC-5 are 0.25, 0.36, 0.42 and 0.39 respectively. The hydrophilicity of the PEC films was examined by using contact angle measurement. When Na-Alg is the outer layer in the PEC, hydrophilicity is higher. Roughness of the film surfaces was characterized by AFM measurements. The solubility of the films was tested in different organic solvents and in aqueous solution of acidic and basic pH values. They are insoluble in water and up to pH=4.2 in acid buffer solution. The swelling properties of the PEC films were studied in acidic aqueous solution of pH value 1.2 and in water. The highest equilibrium % swelling values among the PEC films have been obtained as 215%

and 155% for PEC-5, in water and acidic buffer respectively within an hour. The drug loading-release properties for the PEC were studied using ciprofloxacin HCl as a model drug. The three layer film PEC-3, which is composed of Na-Alg outer layer deposited on a P<sub>4</sub>VP/Na-Alg double layer, is characterized by the lowest roughness ( $R_q=16.3$  nm) and the most hydrophilic surface with a contact angle value of  $38.1^\circ$  among all other films prepared. Its crystallinity index is 0.36, and starts to degrade at  $195^\circ\text{C}$ . It exhibits 130-135% equilibrium swelling capacity in acid buffer and water respectively. PEC-3 is the film with the highest drug loading capacity and drug loading efficiency values of 3.51% and 87% respectively when the initial drug concentration is 12.5 ppm. A cumulative drug release of 65% is obtained from PEC-3 within 24 h in water when the initial concentration of the drug solution is 12.5 ppm. Several kinetic models including zero order, first order, Higuchi and Korsmeyer-Peppas were tested to understand the kinetics and mechanism of the drug release from the PEC films of Na-Alg and P<sub>4</sub>VP. The best fit was obtained with Higuchi's equation. Release mechanism was found to be Fickian according to the Korsmeyer-Peppas equation.

**Keywords:** sodium alginate, poly(4-vinylpyridine), polyelectrolyte complex, multilayer, ciprofloxacin HCl, LbL.

## ÖZ

Sodyum alginat ve poli(4-vinilpiridin) den oluşan çok katmanlı polielektrolit kompleks filmler (PEK), sulu sodyum alginat (Na-Alg) ve 0.1 M HCl çözeltisinin çözügen olarak kullanıldığı asitli poli(4-vinilpiridin) (P<sub>4</sub>VP) çözeltileri ile elde edildi. Na-Alg film sırasıyla P<sub>4</sub>VP, Na-Alg çözeltilerine batırılarak çok katmanlı PEK filmler elde edildi. Na-Alg ve PEK filmlerin morfolojisi, topografisi ve kimyasal yapıları araştırılarak sırasıyla SEM, AFM ve FTIR spektroskopisi yöntemleri ile bulundu. Katman sayısının ve dış katmanın kimliğinin fizikokimyasal özellikleri etkilediği görüldü. PEK filmlerin termal özellikleri TGA yöntemi ile incelendi. Filmlerin ilk bozunma sıcaklığı PEC-2, PEC-3, PEC-4, PEC-5 için sırasıyla 180°C, 195°C, 195°C ve 200°C olarak gözlemlendi. Öte yandan Na-Alg ve P<sub>4</sub>VP filmlerin sırasıyla 215°C ve 290°C sıcaklıkta bozunduğu görüldü. Örneklerin kristallik endeksleri XRD analizi ile bulundu. Polimerler arasında kompleks oluşumunun kristallik oranını düşürdüğü gözlemlendi. Na-Alg filmin kristallik endeksi 0.49 iken bu değer PEC-2, PEC-3, PEC-4 ve PEC-5 için 0.25, 0.36, 0.42 ve 0.39 olarak hesaplandı. Filmlerin hidrofilik karakteri temas açısı ölçümleri ile bulundu. Dış katmanın Na-Alg olması durumunda hidrofilik karakterin arttığı gözlemlendi. Film yüzeyinin pürüzlülüğü AFM ölçümleri ile belirlendi. Filmlerin organik çözücülerde, suda, asidik ve bazik pH değerindeki sulu çözeltilerde çözünürlüğü test edildi; pH-4.2 değerine kadar asitli ortamda çözünmediği görüldü. Filmlerin şişme davranışları suda ve pH-1.2 asitli tampon çözeltide incelendi. PEC-5'in asitte ve suda %215 ve %155 denge şişme değerleri ile en fazla şişme değerine sahip olduğu görüldü. Filmlerin ilaç yükleme ve salım özellikleri siprofloksasin.HCl (CIP.HCl) model bileşik kullanılarak çalışıldı. Na-Alg-P<sub>4</sub>VP-Na-Alg katmanlarında oluşan üç

katmanlı film, PEC-3 filmin en düşük pürüzlülük ( $R_q=16.3$  nm) değerine sahip olduğu, ayrıca  $38.1^\circ$  temas açısı ile en hidrofilik yüzeye sahip olduğu belirlendi. Bu örneğin kristallik endeksi 0.36 dır ve  $195^\circ\text{C}$  sıcaklıkta bozunmaya başlamaktadır. Ayrıca asitli ortamda ve suda %135-130% dengede şişme değerine sahiptir. Bu özelliklere sahip PEC-3 filmin en yüksek CIP.HCl yükleme (3.51%) kapasitesi ve verimliliği (87%) değerlerini verdiği bulundu. PEC-3 filminden 24 saat sonunda suda, ilacın %65'inin salındığı hesaplandı. Salım kinetiği ve mekanizması sıfırıncı dereceden, birinci dereceden, Higuchi ve Korsmeyer-Peppas denklemlerine göre incelendi. Salım kinetiğinin Higuchi denklemine uyduğu salım mekanizmasının ise Korsmeyer-Peppas denklemine göre Fickian olduğu bulundu.

**Anahtar Kelimeler:** sodyum alginat, poli(4-vinilpiridin), polielektrolit kompleks film, siprofloksasin HCl, LbL.

## DEDICATION

*To my lovely Mom and Dad for  
their love and prayers,  
to my sisters and  
my brother*

## ACKNOWLEDGMENT

My deep gratitude first goes to my supervisor Prof. Dr. Elvan Yilmaz for her guidance, advices, unlimited support and for being one of the best and a professional mentor. This work would not be possible without you.

I would also like to thank Prof. Dr. Osman Yilmaz for his kindness, love and encouragement during my PhD journey, with the knowledge and skills I gained from him to be prepared for a successful academic life.

Also the thanks go to my committee members Prof. Dr. Mustafa Gazi and Assoc. Prof. Dr. Terin Adalı for their help, support and recommendations during my study and to jury members Prof. Dr. Gülsen Asman and Prof. Dr. Şadi Şen for their time and sincere efforts to make this humble work better.

Special thanks also go to all my friends, classmates and lab-mates in the department for their support all the time. And all the staff of the chemistry department for being very helpful and professional.

I am also grateful to all of those whom I had the pleasure to work in the faculty of pharmacy; I would especially like to thank Assist. Prof. Dr. Aybike Yektaoğlu and Prof. Dr. Müberra Koşar for the support, the experience and the knowledge I gained during my period of my work.



And to my lovely brothers in N. Cyprus Dr. Mamoon Al Okour, Dr. Karar Shukur and Dr. Faisal Mustafa, your help, support and encouragement gave me the strength to overcome all the difficulties in this journey.

Most importantly, I would like to thank my parents, Dr. Mohammad and Dr. Nawal, my sisters- Lara, Alaa, Rawan, Razan and Mays- and my brother Hamzah for their patience, support and love. Thanks for being in my life.

# TABLE OF CONTENTS

ABSTRACT .....	iii
ÖZ .....	v
DEDICATION .....	vii
ACKNOWLEDGMENT .....	viii
LIST OF TABLES .....	xii
LIST OF FIGURES .....	xiii
1 INTRODUCTION .....	1
1.1 Synthetic and Natural Polymers .....	2
1.2 Hydrogels .....	3
1.2.1 Classifications of hydrogels.....	5
1.3 Polyelectrolytes .....	5
1.3.1 Polyelectrolyte complexes (PEC).....	6
1.3.2 Polyelectrolyte Multilayer Systems.....	9
1.4 Drug Delivery Systems .....	10
1.5 Drug-Release Kinetics.....	12
1.6 Skin Wound Healing .....	13
1.7 Sodium Alginate.....	14
1.8 Poly (4-vinylpyridine) .....	17
1.9 Ciprofloxacin HCl .....	19
2 EXPERIMENTAL .....	21
2.1 Materials .....	21
2.2 Instruments .....	21
2.3 Method .....	22

2.3.1 PEC Film Preparation.....	22
2.3.2 Solubility and Swelling Studies.....	23
2.3.3 Film Thickness and Opacity Measurements.....	23
2.3.4 Drug Loading and Release Experiment.....	23
2.3.5 Drug Release Kinetics .....	25
<b>3 RESULTS AND DISCUSSION .....</b>	<b>27</b>
3.1 Preparations of the PEC and PEC Multilayer Membranes .....	27
3.2 Film Thickness and Opacity Measurements .....	28
3.3 FTIR .....	29
3.4 XRD Analysis .....	30
3.5 Thermal Gravimetric Analysis (TGA) of the Films.....	32
3.6 Scanning Electron Microscopy (SEM) .....	34
3.7 Atomic Force Microscopy (AFM) and Contact Angle (CA) .....	36
3.8 Solubility of PEC Multilayer Films .....	39
3.9 Swelling.....	40
3.10 Drug Loading and Release .....	41
3.10.1 Drug Loading.....	41
3.10.2 In vitro CIP.HCl Release from NaAlg/P <sub>4</sub> VP PEC Films .....	44
3.10.3 Drug Release Kinetics .....	48
<b>4 CONCLUSION .....</b>	<b>55</b>
<b>5 FUTURE WORK.....</b>	<b>56</b>
<b>REFERENCES.....</b>	<b>57</b>

## LIST OF TABLES

Table 1: Examples of some natural polymers with their applications .....	3
Table 2: The PEC multilayer with the outer surface.....	22
Table 3: The thickness and the opacity values of PEC multilayer and NaAlg films .	29
Table 4: The temperature stages of degradation, weight % and the crystallinity indexes of Na-Alg, PEC-2, PEC-3, PEC-4 and PEC-5.....	33
Table 5: Solubility behavior of the PEC multilayers in different solvents .....	40
Table 6: Effect of loading time on the loading efficiency on the different PEC multilayer films at 12.5 ppm concentration .....	42
Table 7: Drug loading capacity and drug loading efficiency of the different PEC multilayers.....	42
Table 8: Cumulative % release values after one day for all PEC samples at 20 and 12.5 ppm concentrations .....	47
Table 9: In vitro dissolution kinetics of ciprofloxacin HCl in 20 and 12.5 ppm in all films .....	50

## LIST OF FIGURES

Figure 1: Scheme of the formation of chemical and physical hydrogels.....	4
Figure 2: Classification of polyelectrolytes .....	6
Figure 3: Classes of the formation of a PEC.....	7
Figure 4: Types of PEC and example to each type .....	8
Figure 5: A scheme of layer-by-layer adsorption of polyelectrolyte .....	10
Figure 6: Chemical structure of sodium alginate .....	14
Figure 7: Methods for the modification of Na-Alg.....	16
Figure 8: The protonation of P <sub>4</sub> VP in acidic medium.....	19
Figure 9: Chemical structure of ciprofloxacin HCl [91].....	20
Figure 10: A schematic representation of the PEC preparation .....	28
Figure 11: The transparent PEC film .....	28
Figure 12: FTIR spectrum of (a) P <sub>4</sub> VP, (b) Na-Alg, (c) PEC-2, (d) PEC-3, (e) PEC-4 and (f) PEC-5 film.....	30
Figure 13: XRD diffractograms of a) NaAlg film, b) PEC-2, c) PEC-3, d) PEC-4 and e) PEC-5 multilayer films .....	31
Figure 14: TGA curves for a) P <sub>4</sub> VP b) Na-Alg c) PEC-2 d) PEC-3 e) PEC-4 f) PEC-5 .....	34
Figure 15: SEM micrographs of a) Na-Alg, b) PEC-2 c) PEC-3 d) PEC-4 and e) PEC-5 multilayer films (5000x magnification) .....	35
Figure 16: AFM analysis (left and middle column) and contact angles (right column) of water droplets of a) NaAlg, b) PEC-2, c) PEC-3, d) PEC-4 and e) PEC-5 .....	38
Figure 17: Contact angles of Na-Alg and the PEC multilayer membranes .....	39

Figure 18: Swelling % for polyelectrolyte multilayers PEC-2, PEC-3, PEC-4 and PEC-5 in a) water and in b) acidic buffer .....	41
Figure 19: Calibration curve for CIP.HCl solution .....	43
Figure 20: SEM pictures for the CIP.HCl loaded multilayers a) in PEC-2 and b) in PEC-3 .....	44
Figure 21: The % cumulative release for a) PEC-2, b) PEC-3, c) PEC-3 and d) PEC-5 in both water and in pH=1.2 buffer solution for 12.5 ppm drug solution .....	46
Figure 22: The % cumulative release for a) PEC-2, b) PEC-3, c) PEC-3 and d) PEC-5 in both water and in pH=1.2 buffer solution .....	47
Figure 23: Zero order kinetics for the release of CIP.HCL from the 20 ppm loaded PEC films in a) water and in b) acid buffer pH=1.2 .....	51
Figure 24: First order kinetics for the release of CIP.HCL from the 20 ppm loaded PEC films in a) water and in b) acid buffer pH=1.2 .....	51
Figure 25: Higuchi kinetics for the release of CIP.HCL from the 20 ppm loaded PEC films in a) water and in b) acid buffer pH=1.2 .....	52
Figure 26: Korsmeyer-Peppas kinetics for the release of CIP.HCL from the 20 ppm loaded PEC films in a) water and in b) acid buffer pH=1.2 .....	52
Figure 27: Zero order kinetics for the release of CIP.HCL from the 12.5 ppm loaded PEC films in a) water and in b) acid buffer pH=1.2 .....	53
Figure 28: First order kinetics for the release of CIP.HCL from the 12.5 ppm loaded PEC films in a) water and in b) acid buffer pH=1.2 .....	53
Figure 29: Higuchi kinetics for the release of CIP.HCL from the 12.5 ppm loaded PEC films in a) water and in b) acid buffer pH=1.2 .....	54
Figure 30: Korsmeyer-Peppas kinetics for the release of CIP.HCL from the 12.5 ppm loaded PEC films in a) water and in b) acid buffer pH=1.2 .....	54

# Chapter 1

## INTRODUCTION

In this study, polyelectrolyte complex (PEC) multilayer films have been prepared by making use of the ionic interaction between Na-Alg and P<sub>4</sub>VP in aqueous solution with the aim of modifying the physicochemical characteristics of sodium alginate for biomedical applications via a green process. Sodium alginate film was used as the substrate to build multilayers of P<sub>4</sub>VP and Na-Alg alternatively on top of each other. The bulk and surface properties of the multilayer Na-Alg/P<sub>4</sub>VP films such as crystallinity, thermal stability, morphology, roughness and wettability, which are critical parameters in biomaterials characterization, have been determined. Investigation of other physicochemical properties of the films reveal that the multilayer Na-Alg/P<sub>4</sub>VP films prepared are thin, transparent, hydrophilic matrices stable in acidic buffer up to pH 4.2. Their solubility and swelling characteristics indicate that these films could act as potential transdermal drug delivery systems for skin wound healing under acidic conditions. Including antibacterial agents in skin wound healing dressings bring an advantage to the system to protect the wound from infections during healing process. Therefore, the Na-Alg/P<sub>4</sub>VP films prepared were used as loading and release matrices for the antibacterial agent CIP.HCl as new films suitable for skin wound healing.

## **1.1 Synthetic and Natural Polymers**

Synthetic polymers are considered as one of the most important materials that played a major role in the industrial revolution in the last few decades. It's dependent upon crude oil and natural gas made this industry economically efficient due to their lower prices. These polymers can resist physical and chemical degradation which affect the ecological system. Since a majority of them are non-biodegradable, synthetic polymers are considered to be one of the main pollutants of the environment and causing serious problems to both ground and surface water [1, 2]. The most popular petroleum based polymers are polyethylene, polystyrene, poly(ethylene terephthalate) and polypropylene. They are mainly used in plastic industries but with the problems of CO<sub>2</sub> emissions and energy requirements [3]. Nowadays, the increasing demand on industry raised the interest of finding a safe, environmentally friendly and renewable replacement of synthetic polymers, to live in a world free of pollution caused by plastics. As an alternative, natural polymers attracted all the attention because they are highly available, renewable, biodegradable, biocompatible and sustainable [3, 4]. Natural polymers are produced either from plant sources, algal sources or from animal origin. Cellulose, gum Arabic, starch and guar gum are examples to natural polymers of plant origin. Galactans, alginates and carrageenan are obtained from algae. Chitin, hyaluronic acid (HA) and glycosaminoglycans are from animal origin. Some of them, such as gellan gum, dextran, xanthan gum and pullulan are obtained from microorganism sources [6,7]. They have got many applications that make them a great alternative for synthetic polymers as summarized in Table 1.



Table 1: Examples of some natural polymers with their applications

<b>Natural polymer</b>	<b>Application</b>	<b>References</b>
Chitosan	Wound healing, tissue engineering, water treatment	[8]
Alginic acid	Drug and protein delivery, wound dressing, heavy metal removal	[7, 8]
Starch	Food packaging, drug delivery	[9, 10]
Cellulose	Scaffolds, biomaterial, water treatment	[11, 12]
Dextran	Protein delivery applications	[15]

The majority of natural polymers oxidize at higher temperatures before they melt. They are soluble in aqueous media. In general, they have poor mechanical properties compared to synthetic polymers. Chemical modification is important for natural polymers to make them more competitive, applicable and to be industrially acceptable compared to the synthetic ones and to enhance their degradation rate. To stabilize the structure of the natural polymer in an aqueous media, crosslinking techniques are applied. Methods such as grafting or copolymerization will enhance both the mechanical properties and the biodegradation rate of the final products. Biodegradable products with different physical properties and morphologies were produced by what is called physical blending. Some advanced technologies were applied for the improvement of natural polymers such as the reinforcement of the natural fibers and the active packaging technology [6, 16].

## **1.2 Hydrogels**

Hydrogels are three dimensional materials consisting of chemically or physically crosslinked polymer chains with the ability to absorb large amounts of water which make them versatile materials for biomedical, pharmaceutical and environmental applications [17]. Figure 1 shows a schematic representation of the formation of

hydrogels. Hydrogels can mimic the natural living tissues because of their porosity, high ability to absorb water and their soft texture. These properties give the hydrogel a wide range of medical applications such as in contact lenses, wound dressings, drug delivery, tissue engineering and hygiene products [18]. Although, chemical cross-linkers are good candidates for the improvement of the mechanical properties of the hydrogels, these cross-linkers are not safe for the environment due to their toxicity [19]. For example, glutaraldehyde, a common cross-linker of natural polymers and mainly of chitosan, may cause health problems such as skin irritation, rhinitis and asthmatic symptoms [20]. To avoid the disadvantages of chemically modified hydrogels such as the toxicity, the high cost and environmental hazards, polyelectrolyte complexes (PEC) of biopolymers that form due to the electrostatic interactions between the polycations and the polyanions may be considered as an alternative [21].

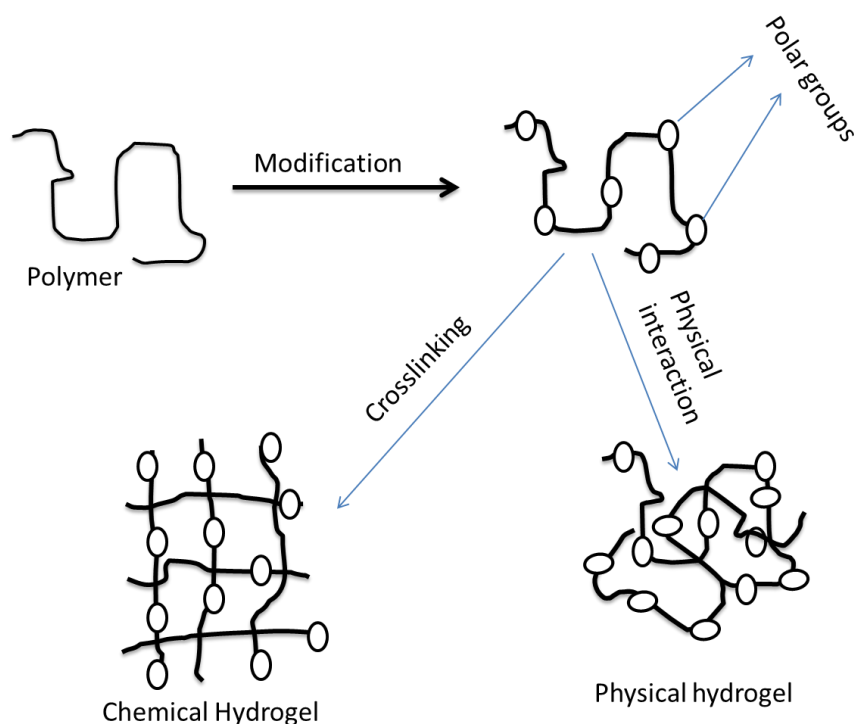


Figure 1: Scheme of the formation of chemical and physical hydrogels

### **1.2.1 Classifications of hydrogels**

Hydrogels and their products can be grouped according to different criteria as shown below:

- 1- According to the source; into natural and synthetic hydrogels [22-24].
- 2- According to the composition of the polymers, this gives different classes of hydrogels such as:
  - a) Homopolymeric hydrogels: composed of one kind of monomers.
  - b) Copolymeric hydrogels: starting from two or more different monomers.
  - c) Interpenetrating polymeric hydrogel (IPN): composed of two different crosslinked polymers.
- 3- According to their configuration:
  - a) Crystalline.
  - b) Semicrystalline.
  - c) Amorphous.
- 4- According to the crosslinking type, chemical and physical.
- 5- According to the form depending on the process of preparation, as film, matrix or microsphere.
- 6- According to electrical charge of the network:
  - a) Neutral (nonionic).
  - b) May include anions or cations (ionic)
  - c) Ampholytic or amphoteric which it contains basic and acidic groups.
  - d) Zwitterionic that contains anions and cations in each repeating unit.

### **1.3 Polyelectrolytes**

Polymers that form polycations or polyanions when dissolved in an ionizing solvent are called polyelectrolytes (PEs). This dissociation will create new electrostatic

interactions between the ionic parts that affect the properties of the polymer such as solubility, diffusion coefficient, pH, ionization constant, viscosity and ionic strength [25]. Polyelectrolytes are classified into various types on the basis of their composition, origin, molecular structure, charge density, the shape and the position of ion sites as summarized in Figure 2.

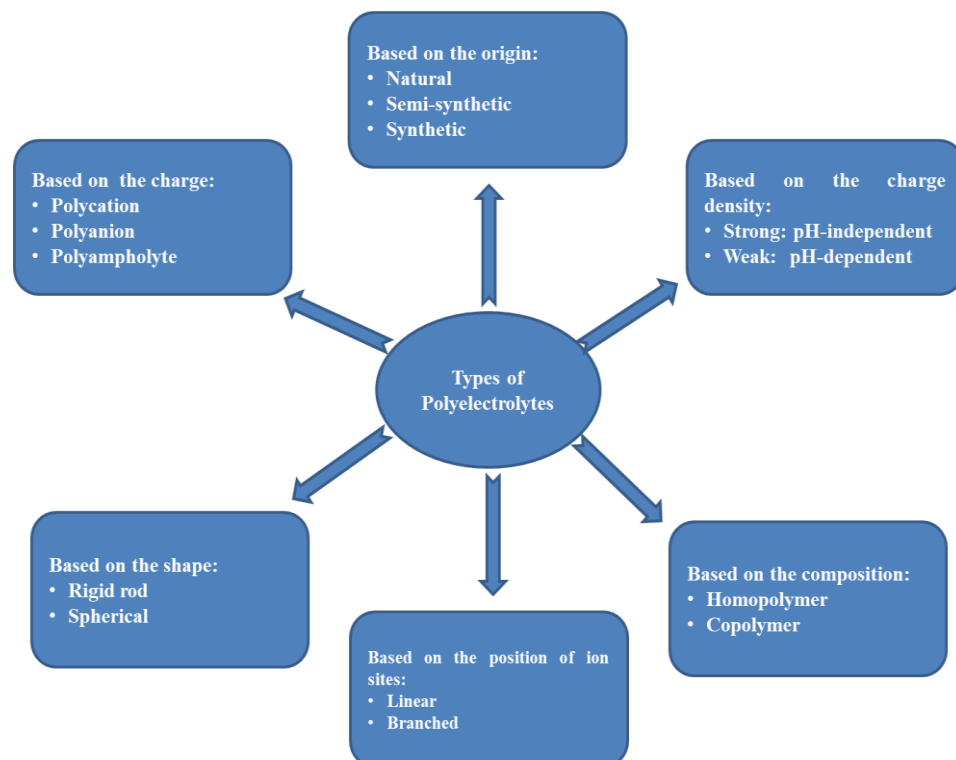


Figure 2: Classification of polyelectrolytes

### 1.3.1 Polyelectrolyte complexes (PEC)

The ionic interaction between the polyanions with the polycations results in the formation of polyelectrolyte complexes (PEC) that differs in their properties from the reacted PEs. Beside the main ionic interaction in forming the PEC, different interactions such as electrostatic, Van der Waals, hydrogen and hydrophobic and coordination bonding can occur between the PEs [26]. The process that leads to the formation of PEC is mainly controlled by the entropy accompanied with the

liberation of ions from the ionic environment surrounding each polyelectrolyte [27]. This ionic interaction will preserve the main properties of the natural polymers such as the biodegradability and low toxicity, and no extra purification is needed as no chemical cross-linker is added. Ionic strength and pH of the PE solutions, the conformation of their chains, temperature and the duration of the complexation, and the concentration of the PE solutions are the main factors that affect the formation of PECs [28]. Figure 3 summarizes the main classes of the formation of a PEC. The 1<sup>st</sup> step shows the formation of a primary complex where the coulombic forces dominate or what is called the secondary binding sources. The 2<sup>nd</sup> step shows the formation of new bonds and/or adjustment of the distorted chains. The 3<sup>rd</sup> step includes the aggregation of secondary complexes, mainly via hydrophobic interactions [29].

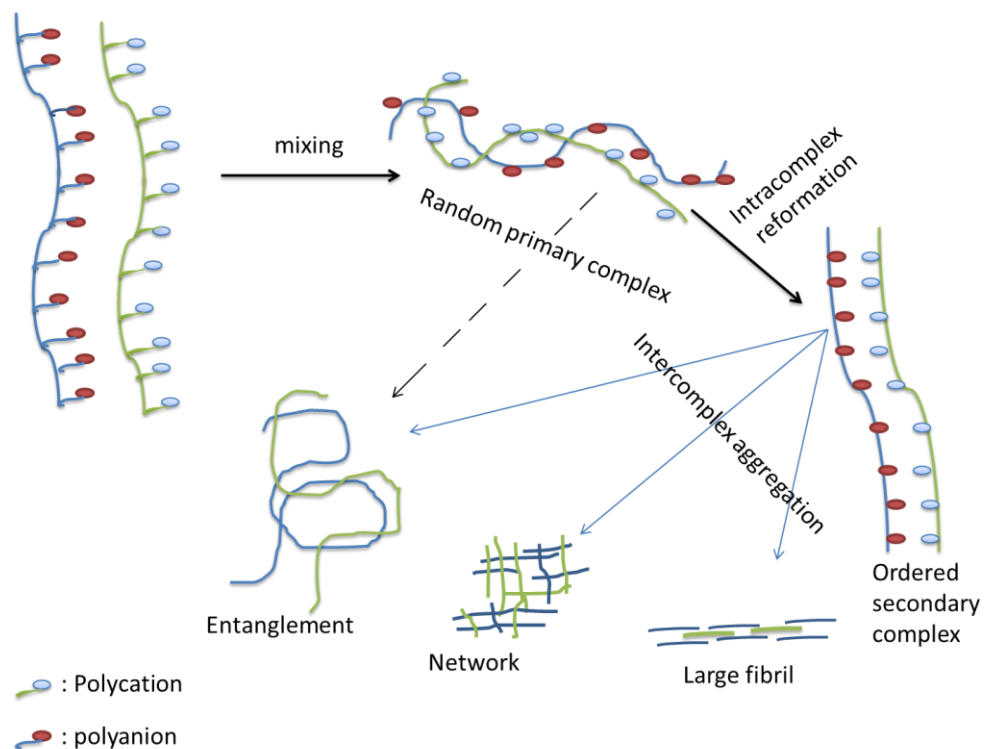


Figure 3: Classes of the formation of a PEC

PECs are versatile materials with a wide range of applications. For example, chitosan-sodium alginate and chitosan-pectin PEC membranes were used as drug delivery systems [30]. Alginate-chitosan-dermatan sulfate PEC was tested in tissue regeneration [31], and chitosan-pectin-alginate as scaffold for tissue engineering [32]. Polyelectrolyte-fluorosurfactant complex was used for oil/water separation in the environmental field [33]. The crystalline nanocellulose/chitosan/carboxymethyl cellulose PEC was applied in food packaging [34]. Figure 4 shows the different types of PECs that formed based on the types of PE used; when both PEs from natural source such as chitosan with alginate, natural with synthetic PEs as in gelatin-sodium carboxymethyl cellulose, when both PEs are synthetic such as poly (vinylbenzyltrimethyl -ammonium chloride) and poly (methacrylic acid), PECs from surfactants and polyions an example is dodecyl dimethylammonium bromides (12-2-12) with anionic polyelectrolytes and protein polyelectrolyte complexes as in bovine serum albumin with poly (diallyl dimethylammonium chloride) [29].

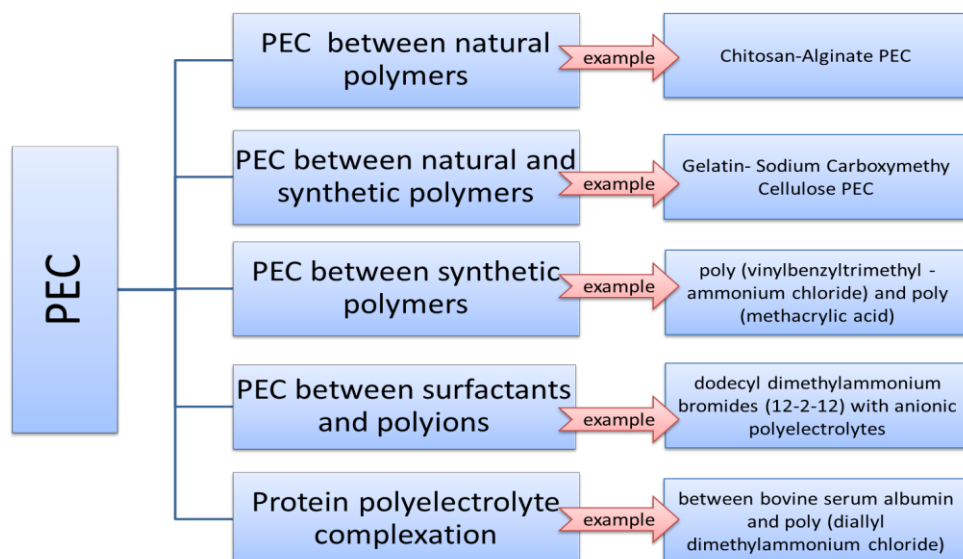


Figure 4: Types of PEC and example to each type

### 1.3.2 Polyelectrolyte Multilayer Systems

The alternating adsorption of the oppositely charged PEs will result in the formation of what is called multilayer polyelectrolytes. This method allows formation of ultrathin functional membranes [35]. Polyelectrolyte multilayers (PEM) are firstly formed by the electrostatic interaction between the PEs. Then the layers will be built up by the alternative adsorption of the polymers. Each adsorption step will invert the charge of the surface to offer strong electrostatic forces leading to the formation of a stable layered complex [36]. Later, with more step-by-step addition of PEs, other types of interactions such as covalent bonding and hydrogen bonding between macromolecules will occur beside electrostatic interactions [37]. Figure 5 illustrates the formation of the polyelectrolyte multilayer system, the electrostatic interaction occurs by immersing polyanions and polycations with a charged substrate in a dilute solution of a polyelectrolyte. Layer-by-layer (LbL) method is one of the major and simplest techniques for the preparation of thin films with controlled structures. The preparation procedure of a multilayer component is simple. Immersing of a negatively charged PE substrate into another positively charged PE solution and then rinse it with water to remove the weakly adsorbed PE from the substrate will result a positively charged surface of the substrate due to the adsorption and overcompensation of PE with opposite charges. Adding another negatively charged PE will reverse the net charge of the substrate's surface. By doing these depositions alternatively between the PEs, multilayer films with desirable structures and thicknesses can be achieved [38]. Different forces can be included in the assembly such as hydrophobic interactions, hydrogen bonding and host-guest interactions when the different species and biological molecules have been used to form multilayer films from polysaccharides, polypeptides, lipids, proteins, viruses and

nucleic acids [39]. PEMs nowadays attracted much attention due to its versatility and simplicity. This technique is also useful in allowing nanoscale control of the structure, the thickness and the composition of the membranes. These PEMs can be prepared as flat membranes and also as clear hollow capsules. Their structure depends on the polarity, ionic strength and pH of the solution. PEMs are useful in many applications, for example in the field of drug delivery, in microsensors and in microreactors [40], as separating membranes [41], as nonlinear optics, bioadhesion, light-emitting devices, conductive coatings, separations, sensors and patterning [42]. Building the multilayer films from bioresorbable and biocompatible PEs has led to the improvement of cell adhesion on tissue, surfaces and skin-bonding films, the directly applied coatings to endothelial or epithelial cell layers *in situ*, or even coatings on living single cells [43].

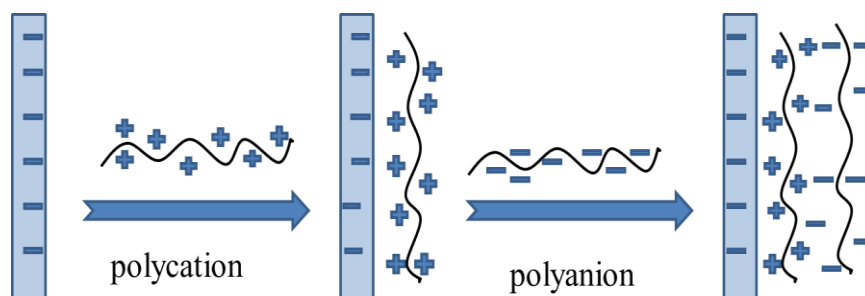


Figure 5: A scheme of layer-by-layer adsorption of polyelectrolyte

## 1.4 Drug Delivery Systems

Drug delivery is a system, which includes methods, technologies, and formulations to carry the medicine to the appropriate site in the body safely, selectively and efficiently and in required amounts. Drug carriers transfer the drug to the required site either by slow release over a sufficiently long period of time or the drug release can be stimulated by some environmental factors such as light, heat and/or pH



changes [44]. Some drugs that have low bioavailabilities, poor water solubilities, or poor membrane permeabilities can be delivered to the target site safely and effectively by using drug carriers. Nowadays, polymer systems are used to develop the drug delivery research and to match their target, the polymer to be used in drug delivery should be non-toxic, biocompatible, non-carcinogenic, non-mutagenic, non-immunogenic and non-teratogenic. The incorporation of drugs into polymer systems has been started in the 50's of the former century for the agricultural products. In the 60's of the same century such methods were applied to the medicinal field by placing the drugs inside silicone rubber tubing or polyethylene matrix as initial studies. In the 70's of the same century for drugs with molecular weight higher than 600 g/mole, ethylene-vinyl acetate copolymer was successfully used as a carrier with a continues release [45, 46].

The use of hydrogels is widely applied in the literature due to the fascinating properties of hydrogels. Its sensitivity toward the environmental conditions such as temperature, pH, glucose, electric signal and light responsive hydrogels with their examples; poly(N-isopropylacrylamide) (PNIPAAm) with acrylic acid monomers, the grafted poly(methacrylic acid) (PMA) with poly(ethylene glycol) (PEG), poly(methacrylic acid-co-butyl methacrylate), poly(2-acrylamido-2-methylpropane sulfonic acid-co-n-butylmethacrylate), and triphenylmethane leuco derivatives under UV respectively [47].

Multilayers made of polymers and biopolymers in the LbL manner, showed good applications in the drug delivery field because of their simplicity and biocompatibility. Many PEs (synthetic or natural) were used in the preparation of PEM as a drug carrier such as gelatin A, chitosan and dextran amine are all

positively charged ones, and some negatively PEs are gelatin B, sodium alginate and dextran sulfate [48]. In the transcutaneous drug delivery, the multilayer films are able to conformally coat on a wide range of substrates that are applied in large-scale delivery therapeutic in an attractive area such as the skin, where multilayer films are able to load drugs and regulate their release over long periods of time [43].

## **1.5 Drug-Release Kinetics**

Drug delivery systems have been designed to control the release dosages that help in the prediction of the exact amount released from the system and to understand the behavior of the release profile, including the transportation of the drug. A biocompatible drug system with a high control release capacity is considered as an effective system [49]. Mathematical models have been proposed in order to understand the mechanisms controlling drug release and to help in developing the product of drug delivery systems. These modeling will reduce the trails of experiments and hence, the cost. In the control of drug release from the dosage, mass could transport via different types of processes. These processes might include the diffusion of water into the system, the diffusion of the drug out of the system, the dissolution of drug, osmotic effect, the erosion of the matrix and polymer swelling [50]. The properties of the drug can influence the release kinetics, such as, the kind of drug, the crystallinity, the solubility, the size of the particles and the dosage amount. Models have been developed to make a comparison in the dissolution profiles of different drugs. The zero order kinetics is modified for some transdermal applications and applied for low solubility drugs, and is applied for slow release profile. First order kinetics is applied for the water soluble drugs in a porous matrix, the release of the drug depends on the amount of drug in the matrix [51]. Many other mathematical models such as Higuchi's model, Hixson–Crowell model, Ritger–

Peppas and Korsmeyer–Peppas model (Power law), Brazel and Peppas model and Baker and Lonsdale model have been developed [52].

## **1.6 Skin Wound Healing**

Skin is the biggest organ in our bodies and forms a barrier that protects against the external environment, preventing the bacteria and viruses from entering into the body and helping in keeping a controlled body temperature and maintains its hydration. An injury to the skin may create a crack that allows bacteria to enter and cause a wound infection and as a result an inflammation. Any break in the skin reaching the epidermis will cause the tissues to lose fluids. Wounds could lead to death if it reached 10% and above of the body surface area due to the loss of the extracellular fluid [53].

The main goal with any wound treatment is to attain healing faster and in a simple way, with the secondary goal of reducing the formation of scars. Healing of wounds depends on factors such as the injury's nature that caused the wound, the time, whether a chronic or acute, and how deep is the injury to both skin and the tissue beneath. Those factors describe wounds and give evaluation of the final healing but not a standard classification and as a result these factors will affect the wound's ability to heal with or without surgery [54]. Nutritional or biochemical imbalances and diabetes may delay wound healing [55]. Besides, the depth of the wound can affect skin wound healing. The damage to the skin can be grouped into three as superficial, deep dermal or full thickness. The wound is protected from infection and contamination by using wound dressings. This physical barrier would keep the wound safe from the outer environment. A good dressing will not stick to the wound, but it will allow the exchange of gases and will keep moisturizing the wound [56].

With the presence of the vehicle the active ingredient is delivered to the target organ, where the required effect is attained. There is a wide range of polymers as vehicles to the target organs including the skin. Polymers can be gel systems and also found in creams and emulsions. Polymers act as matrix in wound dressings and patches and in transdermal systems they are used as skin adhesives. Besides, polymers can maintain the supersaturation and enhance the penetration. Examples of applied polymers on skin are cellulose derivatives, carageenan, chitosan, polyvinylalcohol, polyacrylates, silicones and polyvinylpyrrolidone [57].

### 1.7 Sodium Alginate

Sodium alginate (Na-Alg) is a water soluble biopolymer forming 40 % of the dry mass of three different kinds of brown algae, *Ascophyllum nodosum*, *Laminaria hyperborean* and *Macrocystis pyrifera*. It can also be isolated from bacterial sources. Na-Alg is an abundant, biodegradable, non-immunogenic, biocompatible and a nontoxic polyelectrolyte composed of the linear and flexible part  $\beta$ -D-mannuronic acid (M blocks) and the branched part  $\alpha$ -L-guluronic acid (G blocks) that offers the stiffness conformation of Na-Alg [58]. Figure 6 shows the general structure of sodium alginate.

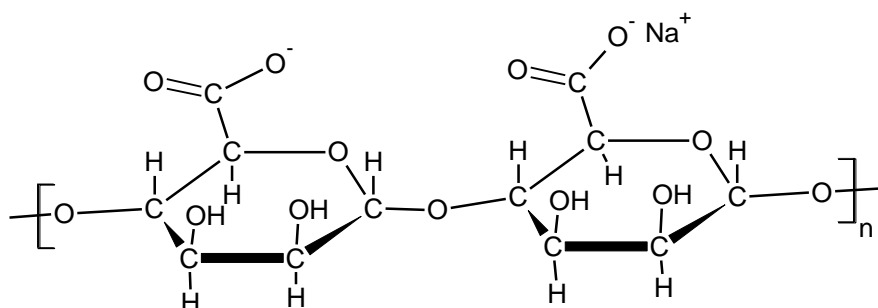


Figure 6: Chemical structure of sodium alginate

Storing Na-Alg in the powder form in a dry, cool and dark place will prevent it from degradation for few months and it could be few years if the storage is done in the freezer. Alginate is able to degrade by the effect of strongly basic media ( $\text{pH} > 10$ ) and by enzymatic effect like the enzyme lyase via beta-elimination mechanism leaving unsaturated compounds as a result of both ways. When the pH is lower than 5 this will lead to the degradation of alginate by a process called "acid catalyzed hydrolysis". In addition, heat treatment, irradiation and autoclaving ethylene oxide treatment all can affect alginate to be degraded [59].

Crosslinking of Na-Alg is an important process to form hydrogels of the biopolymer. Gel formation is done by the crosslinking reaction with  $\text{Ca}^{2+}$ ,  $\text{Ba}^{2+}$  and  $\text{Sr}^{2+}$ , this gelation is described by the "egg-box" model in which the divalent cations are coordinately bounded to the carboxylates of guluronic acid. On the other the monovalent cations are not able to form gels with Na-Alg [60]. Also glutaraldehyde is another cross-linker for Na-Alg to be used in the pervaporation separations of ethanol–water mixtures [61]. Dissolving Na-Alg in water will give a polyanion able to make a complex with another cation and/or polycation to form polyelectrolyte complex (PEC) used in the delivery of protein drugs [62]. Modification methods of alginates are shown in Figure 7. Modification via acetylation, this has been done by Wassermann who used the gaseous reagent ketene to enhance the properties of the polymer and helped in avoiding the degradation problems [63]. Phosphorylation using urea and phosphoric acid has been described to synthesize derivatives of phosphorylated alginates that show better resistance to degradation by comparing with the crosslinked alginate in regards to degradation by chelating agents [64]. Modification by grafting with poly(acrylonitrile) (PAN) using ceric ammonium nitrate (CAN) as initiator gives alginate a hydrophobic nature that slow down the

erosion and dissolution rates of the polysaccharide backbone. [65]. Sulfation of sodium alginate has been reported by Yumin et al using chlorosulfonic acid in formamide. This modification show good anticoagulant activity and blood compatibility [66]. A hydrophobic modification has been done by Hubert et al to reduce or prevent the high water solubility of sodium alginate, in this modification short polyether chains were covalently attached to the backbone of sodium alginate [67].

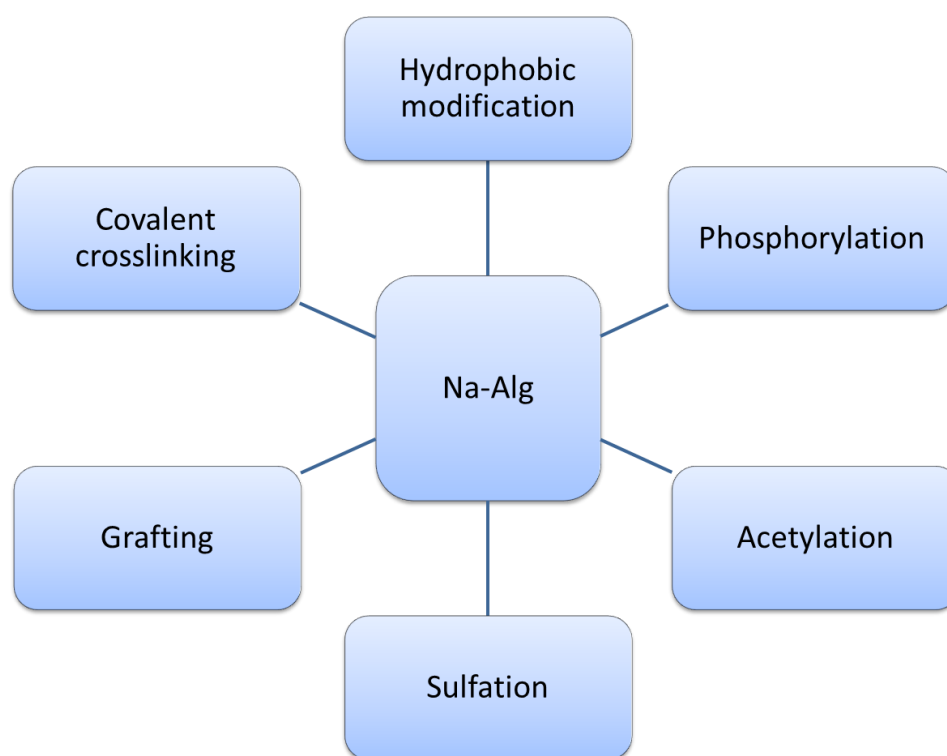


Figure 7: Methods for the modification of Na-Alg

This diversity in the modification of Na-Alg, the availability in different grades and the cheap price, makes this polymer highly demanded in many applications. It can be used in the form of plain and coated beads in the entrapment of proteins such as heparin, melatonin, vaccines and hemoglobin, and as microspheres in oral delivery systems. Also, alginate is suitable for biomolecules delivery to mucosal tissues due

to the mucoadhesive property of the polymer. Alginate blends with other polymers such as alginate/chitosan blends are also of great importance in the drug release applications [68]. The hydrophilicity and biocompatibility make the alginate a suitable polymer in many medical applications including wound dressings. The hydrophilic alginate gels with its high absorption ability limits wound exudations and reduces bacterial contamination [69]. An ion exchange reaction between calcium from the alginate hydrophilic gel with the sodium and the exudates in the blood will produce a soluble calcium-sodium alginate, in which calcium ions will be released very fast, thus giving an important factor of the coagulation cascade. Studies demonstrated that calcium alginate is able to diminish the bleeding of torn skin [70]. Silk fibroin and alginate blended sponge (SF/AA-blended sponge) is one of the alginate gels that is working as a wound dresser since its able to absorb moisture and keep an appropriate moist environment that promotes a fine wound healing [71]. The stimulation of monocytes by alginate helps in the production of high levels of cytokines such as tumor necrosis factor- $\alpha$  and interleukin-6 which in turn will improve wound healing [72].

### **1.8 Poly (4-vinylpyridine)**

Poly (4-vinylpyridine) ( $P_4VP$ ) bearing unique properties such as its basicity and hydrophilic-hydrophobic balance provide this polymer with characteristics to be used in many applications such as an antimicrobial materials, a host/ligand of metal-containing chromophores, sensors and actuators and in the adsorption of metals such as  $Cu^{2+}$ . [73].  $P_4VP$  is considered as a weak base and insoluble in water but soluble in HCl solution forming a protonated polymer, a pyridonium ion. It is a pH sensitive polymer where it shows good solubility at pH values lower than 4.7. It becomes insoluble at pH values greater than 4.7.  $P_4VP$  swells in toluene, benzene and xylene,

and is soluble in ethanol, methanol, pyridine, propanol, benzyl alcohol and cyclohexanol. It is insoluble in diphenyl ether, ethyl ether, acetone, dioxane, petroleum ether and ethyl acetate [74]. Block copolymers that contain P<sub>4</sub>VP have the ability to coordinate with metals and self-assemble into different supramolecular structures. P<sub>4</sub>VP can form a pH responsive micelles aiming to controlled release of drugs. One example is the triblock copolymer made of poly (ethylene glycol) (PEG) and P<sub>4</sub>VP (P<sub>4</sub>VP-*block*-PEG-*block*-P<sub>4</sub>VP) loaded with gold to be used as a drug carrier for the treatment of different cancers. The copolymer proved to have no cytotoxicity on both cancerous and non-cancerous cells [75]. P<sub>4</sub>VP nanoparticles were used in both medical and environmental applications; as a drug release system for naproxen sodium salt as the drug model and for the removal of organic contaminants from water where phenol used as the model contaminant [76]. Due to its segmented block copolymer character, poly(4-vinylpyridine-*co*-styrene) is considered as one of the most extensively used polymer group of biomaterials applied for medical implants [77].

Quaternization of P<sub>4</sub>VP gives the polymer the ability to form PEC with other polyanions. This quaternization is done either by protonation as shown in Figure 8 or by the nucleophilic attack on alkyl halide [78]. Many applications for the quaternized P<sub>4</sub>VP (QP<sub>4</sub>VP) mentioned in the literature are in regards to the environmental field like the ability to remove metal ions from groundwater such as copper [79] and mercury [80]. Furthermore, it is reported in the literature that the antibacterial activity of the QP<sub>4</sub>VP plays an important role in wound dressing applications [81].



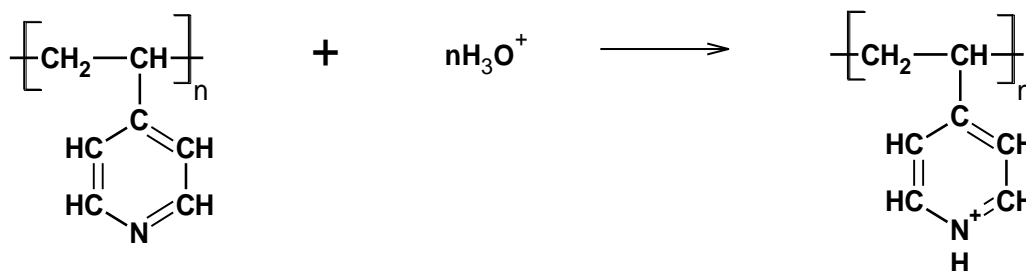


Figure 8: The protonation of P<sub>4</sub>VP in acidic medium

The ability of P<sub>4</sub>VP in forming PECs was also studied, that cationic PE of the protonated P<sub>4</sub>VP using hydrochloric acid is complexed with the anionic PE sulfonated polyaniline (SPANI) giving a precipitate of a gel-like material [82]. Forming a multilayer system depending on the formation of hydrogen bonding has been investigated using poly acrylic acid (PAA) and P<sub>4</sub>VP [83]. And forming a PEC multilayers by the layer-by-layer (LbL) assembly made of poly(N-octyl-4-vinyl pyridinium iodide) and poly(styrene sulfonate) to be used in control corrosion application [84].

### 1.9 Ciprofloxacin HCl

Ciprofloxacin hydrochloride (CIP) is a highly effective antibiotic against both gram negative and gram positive bacteria. It is a derivative of the quinolone-carboxylic acid family. CIP is a widely used drug in the world, its antibacterial activity makes it effective in the treatment of so many infections such as lower respiratory tract infections, bone and joint infections, urinary tract infections and infectious diarrhea [85]. With two proton binding sites, this drug is considered as a zwitterionic molecule, this property makes it highly soluble in water and in acidic medium in lower degree [86]. Figure 9 shows the chemical structure of CIP. Many works was done on the drug delivery/release of CIP using different polymer/biopolymer materials as carriers. For example, CIP was complexed through the amine group with the carboxylic part from the dendronized polymer in the treatment of mucosal and

topical opportunistic infections in both human or veterinary applications [87]. The loading of CIP using chitosan and pectin microspheres by a spray-drying technique to be used in the treatment osteomyelitis [88], preparing *a situ* gelling system made of Na-Alg and carbopol polymers as a CIP carrier [89], gelatin-Na-Alg PEC was also used as a CIP carrier [90].

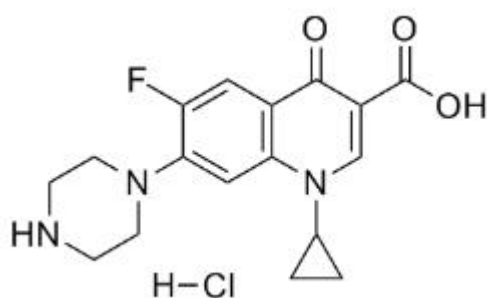


Figure 9: Chemical structure of ciprofloxacin HCl [91]

## Chapter 2

### EXPERIMENTAL

#### 2.1 Materials

Alginic acid sodium salt powder (Aldrich), poly(4-vinylpyridine) (Aldrich), hydrochloric acid (Merck), were used as received. Buffer solution used in this work was prepared using potassium chloride (Aldrich) and hydrochloric acid (Aldrich). Ciproloxacin.HCl was obtained from Pharma Mondial, N.Cyprus.

#### 2.2 Instruments

The films were characterized by scanning electron microscope (SEM) for the observation of the surface morphology using Quanta 400F field Au-Pd coating. Thermal gravimetric analysis (TGA) was used to study the decomposition behavior and the stability of the films using Perkin Elmer Diamond Differential Calorimeter and Perkin Elmer Pyris 1. The study was carried out under N<sub>2</sub> atmosphere at 10 °C min<sup>-1</sup> heating rate. Atomic force microscopy (AFM) using Veeco MultiMode V instrument to study the surface topography, contact angle (CA) to study the wettability of the multilayer films using Attension Theta instrument, and X-Ray diffraction (XRD) using Rigaku Ultima IV X-ray diffractometer were used. All of the analyses given above were performed at METU Central Laboratory in Ankara. The infrared absorption spectra (FTIR) were taken using a Perkin Elmer Spectrum-Two spectrophotometer at Eastern Mediterranean University.

## 2.3 Method

### 2.3.1 PEC Film Preparation

Solutions of each polymer with 1% (w/v) concentration were prepared by dissolving 1.00 g of P<sub>4</sub>VP in 100 mL of 0.10 M HCl solution and the same amount of Na-alginate in 100 mL distilled water.

Films of sodium alginate and sodium alginate/poly (4-vinylpyridine) polyelectrolyte complex (PEC) have been prepared at room temperature. 3.0 mL of 1.0% sodium alginate solution was poured into a glass petri dish (75 x 17 mm) and was left to dry overnight. Then, 3.0 mL of 1.0% P<sub>4</sub>VP solution was added into the Petri dish and the Na-Alg film was dipped into the acidic P<sub>4</sub>VP solution. After 20 minutes contact time to allow complex formation between the polymers, the PEC film obtained was washed with distilled water and left to dry in the oven at 40 °C. To prepare the multilayer films, the same procedure for the formation of the first PEC (denoted as PEC-2) was applied. PEC-2 was dipped into another 3.0 mL of the 1.0% Na-Alg to form PEC-3. Then, 3.0 mL of 1.0% P<sub>4</sub>VP solution was used on PEC-3 to form PEC-4. Finally, PEC-5 was obtained by dipping PEC-4 into 3.0 mL of the 1.0% Na-Alg solution. Each film was rinsed with distilled water before building a new layer on it. Layers were built without drying the parent film. Table 2 shows the outer layer of each PEC multilayer film formed.

Table 2: The PEC multilayer with the outer surface

<b>PEC multilayer</b>	<b>The outer surface of the PEC multilayer</b>
<b>PEC-2</b>	P <sub>4</sub> VP
<b>PEC-3</b>	Na-Alg
<b>PEC-4</b>	P <sub>4</sub> VP
<b>PEC-5</b>	Na-Alg

### 2.3.2 Solubility and Swelling Studies

To determine the film solubility, the samples were immersed in different solvents for 24 hours and the solubility was observed. For the swelling ability of the samples, the dried film has been immersed in water and in HCl/KCl buffer solution pH=1.2 for different time intervals and wiped using a filter paper and then the weight of the film was taken. The measurements were repeated three times. The swelling degree was calculated by using the following equation [92]:

$$\% \text{ swelling} = \left( \frac{W_0 - W_d}{W_d} \right) \times 100 \quad (1)$$

where  $W_0$  is the weight of the wet sample, and  $W_d$  is the weight of the dry sample.

### 2.3.3 Film Thickness and Opacity Measurements

The thickness of the films was measured using a Moore & Wright micrometer. For each sample 5 measurements were taken from random positions on the film and the mean values were recorded. Opacity of the PEC multilayers was evaluated according to the method in Abdollahi et al [93]. The films were cut into stripes and placed in a spectrophotometer cuvette. An empty cuvette was used as the blank and the absorbance was measured at 600 nm. The opacity of the films was calculated according to the following formula:

$$T = \frac{A_{600}}{t} \quad (2)$$

where T is the transparency,  $A_{600}$  is the absorbance at 600 nm and t is the thickness of the film in mm. From this equation the higher the value of T is the lower the transparency and as a result a higher opacity.

### 2.3.4 Drug Loading and Release Experiment

For this part of the study, the antibacterial CIP.HCl has been chosen as the model drug. The loading part was carried out by immersing the PEC films in 25 mL of 12.5 ppm and 20.0 ppm CIP.HCl solutions for 48 hours. Then, using the UV/visible

spectrophotometer at 275 nm, the absorbance of the solutions has been taken and the amount of drug loaded is calculated from the calibration curve. The drug loading efficiency (DLE) and the drug loading capacity (DLC) have been calculated according to the following equations:

$$DLE = \frac{W_d}{W_t} \times 100\% \quad (3)$$

where  $W_d$  is the weight of loaded drug, And  $W_t$  is the weight of drug in feed.

$$DLC = \frac{W_d}{W_T} \times 100\% \quad (4)$$

where  $W_d$  is the weight of loaded drug, and  $W_T$  is the weight of the PEC.

Release experiments were performed by immersing CIP.HCl loaded membranes in beakers filled with 50 mL of medium solutions (pH 1.2 and distilled water). The temperature was kept at 37 °C. At predetermined intervals of the *in vitro* release experiment, 3.0 mL of the medium solution was removed from the beaker and the concentration of ciprofloxacin HCl released was measured using a UV–vis spectrophotometer at  $\lambda_{\max} = 275$  nm wavelength. The amount of cumulative release was determined from interpolation of standard calibration curve at  $\lambda_{\max} = 275$  nm using the following formula:

$$\text{Cumulative percent release} = \frac{Q_t}{Q_m} \times 100\% \quad (5)$$

where  $Q_t$  is the amount of CIP.HCl released from the film at time t and  $Q_m$  is the total amount of CIP.HCl loaded onto the PEC.

### 2.3.5 Drug Release Kinetics

The release kinetics of CIP.HCl from the PEC multilayers were studied by using zero order rate, Higuchi, first order and Korsmeyer-Peppas kinetic models with their equations given below:

Zero order rate equation:

$$Q_t = Q_0 + K_0 t \quad (6)$$

where  $Q_t$  is the amount of drug dissolved in time " t ",  $Q_0$  is the initial amount of drug in solution and  $K_0$  is the rate constant of the release.

First order rate equation:

$$\log Q_t = \log Q_0 - \frac{Kt}{2.303} \quad (7)$$

where  $Q_0$  is the initial amount of drug,  $Q_t$  is the amount of drug released at time " t " and  $K$  is first order release constant.

Higuchi's equation:

$$Q = K_H t^{1/2} \quad (8)$$

And Higuchi dissolution constant:

$$K_H = A \sqrt{(2C_{ini} - C_s) D C_s} \quad (9)$$

where  $Q$  is the amount of drug released in time  $t$  per unit area,  $K_H$  is Higuchi dissolution constant.  $A$  is the amount of drug released,  $C_{ini}$  is the initial drug concentration,  $C_s$  is the drug solubility and  $D$  is the diffusivity of the drug in the matrix.

Korsmeyer-Peppas equation:

$$\log \frac{Q_t}{Q} = \log K_m + n \log t \quad (10)$$

where  $Q_t$  is the amount of drug released at time  $t$ ,  $Q$  is the total of drug loaded in the matrix,  $K_m$  is the release rate constant,  $n$  is the release or diffusion constant and  $t$  is time in minutes.



## Chapter 3

### RESULTS AND DISCUSSION

#### 3.1 Preparations of the PEC and PEC Multilayer Membranes

Na-Alg is the salt form of alginic acid and bears free carboxylate ion groups when dissolved in water. Therefore, it acts as an anionic polyelectrolyte in aqueous solution. P<sub>4</sub>VP, on the other hand is a basic polymer due to the presence of the pyridine group in the chemical structure. When it is dissolved in aqueous acid solution, which is hydrochloric acid in this case, the nitrogen atom on pyridine ring is protonated. Hence, P<sub>4</sub>VP acts as a cationic polyelectrolyte in aqueous solution. When these two solutions are mixed together polymer chains bearing opposite charges precipitate out of solution as a complex due to the electrostatic attraction between the polyanion and the polycation. The complexation reaction between Na-Alg and protonated P<sub>4</sub>VP is shown in Figure 10. The multilayer PEC films were prepared by making use of the ionic interaction between the negatively charged carboxyl residues of alginate and the cationic amino groups of the protonated P<sub>4</sub>VP polymers as explained above. The Na-Alg film recovered from aqueous solution contains carboxylate ion functionalities accompanied with Na<sup>+</sup> ions. When the film is dipped into the acidic solution of P<sub>4</sub>VP, the polycation deposits as a thin layer on the Na-Alg film via electrostatic interaction. New layers are built upon each other making use of the same principle. The PEC films obtained are homogeneous and transparent as illustrated in Figure 11.

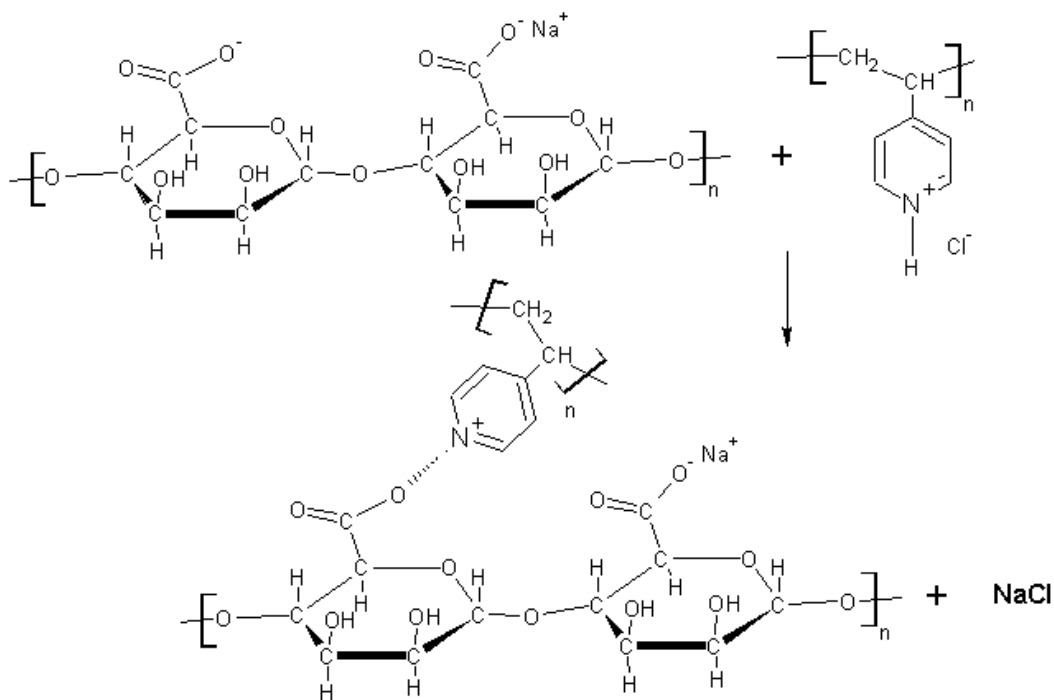


Figure 10: A schematic representation of the PEC preparation



Figure 11: The transparent PEC film

### 3.2 Film Thickness and Opacity Measurements

Opacity is a measurement used to find the transparency of the film. Table 3 shows the thickness and the opacity of Na-Alg and the PEC multilayer films. The lower opacity value of Na-Alg indicates high transparency and homogeneity of the film.

The thickness of the films is of the order of 10  $\mu\text{m}$ . This is the overall thickness of the film including all layers. The thickness of each new layer added on top of each other could not be measured as the precision of the instrument used was of the order of micrometers. More precise measurements are needed to give an explanation for the variations in thicknesses of the films. PEC multilayer films are more opaque (10.3-20.3) than the Na-Alg film (4.46) due to their multilayered nature.

Table 3: The thickness and the opacity values of PEC multilayer and NaAlg films

<b>PEC multilayer</b>	<b>A<sub>600</sub></b>	<b>Thickness (mm)</b>	<b>Opacity (T)</b>
<b>Na-Alg</b>	0.058	0.013	4.46
<b>PEC-2</b>	0.103	0.010	10.3
<b>PEC-3</b>	0.129	0.010	12.9
<b>PEC-4</b>	0.223	0.011	20.3
<b>PEC-5</b>	0.155	0.013	11.9

### 3.3 FTIR

FTIR spectra of P<sub>4</sub>VP, Na-Alg and the PEC films PEC-2, PEC-3, PEC-4 and PEC-5 are shown in Figure 12 a, b, c, d, e and f respectively. In the FTIR spectrum of the P<sub>4</sub>VP film shown in Figure 12 (a) the bands at 1634, 1607, and 1503  $\text{cm}^{-1}$  refer to the stretching vibrations of  $\text{NR}^{4+}$ ,  $\text{C}=\text{N}$ , and  $\text{C}=\text{C}$  (pyridine ring). The peak at 2604  $\text{cm}^{-1}$  refers to the amine salt. In the case of Na-Alg film, spectrum is given in Figure 12 (b), the broad peak from 3100- 3350  $\text{cm}^{-1}$  is attributed to -OH stretching vibration and the vibration peak at 2928  $\text{cm}^{-1}$  is due to C-H stretching. The peaks at 1595  $\text{cm}^{-1}$  and at 1406  $\text{cm}^{-1}$  represent  $-\text{COO}^-$  asymmetric and symmetric- $\text{COO}^-$  stretching respectively. At 1024  $\text{cm}^{-1}$ , -C-O- stretching is observed. The spectra of the PEC multilayer films are shown in Figure 11 c, d, e and f. The band at 1637  $\text{cm}^{-1}$  confirms the electrostatic interaction between the  $-\text{CH}_2\text{COO}^-$  groups of alginate and the

protonated amine in P<sub>4</sub>VP. The new band was assigned to the asymmetrical vibration of the –COO<sup>–</sup> of alginate, resulting from the shift in carbonyl groups of Na-Alg [94]. Furthermore, the peak at 2604 cm<sup>–1</sup> of the amine salt does not exist in the spectrum of the PEC films providing further evidence for complex formation between the two polymers [95].

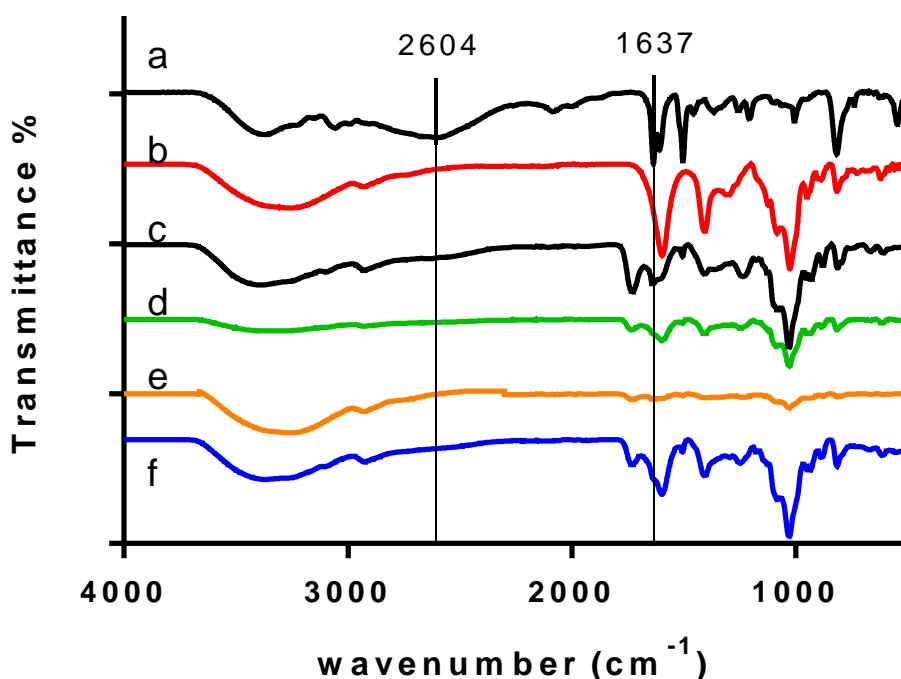


Figure 12: FTIR spectrum of (a) P4VP, (b) Na-Alg, (c) PEC-2, (d) PEC-3, (e) PEC-4 and (f) PEC-5 film

### 3.4 XRD Analysis

The XRD diffractograms of Na-Alg, PEC-2, PEC-3, PEC-4, and PEC-5 are shown in Figure 13 a, b, c, d, and e respectively. The films show characteristic diffraction peaks of Na-Alg at 13° and 21° 2θ angles [96]. The crystallinity index of each sample was calculated using equation 11. The main diffraction peak at 21° was taken as the crystalline peak and 15° was taken as the reference angle to account for the intensity of the amorphous regions.

$$CI = \frac{I_c - I_a}{I_a} \quad (11)$$

where  $I_c$  is the intensity of the crystalline regions and  $I_a$  is the intensity of the amorphous ones.

It was found out that Na-Alg film has the highest crystallinity index value with 0.49. Upon interaction with positively charged P<sub>4</sub>VP, the crystallinity index decreases drastically to 0.23 for PEC-2. The hydrogen bonding interaction among alginate chains is disrupted due to reorientation of the chains after ionic complexation with the positively charged P<sub>4</sub>VP chains. PEC-3, PEC-4 and PEC-5 have comparable crystallinity index values to each other calculated as 0.36, 0.42 and 0.39. These values are lower than that of pure Na-Alg, but higher than the crystallinity index of PEC-2. The reason for this should be the contribution of free Na-Alg chain segments not involved in ionic interactions to the formation of crystalline regions in the multilayered structures.

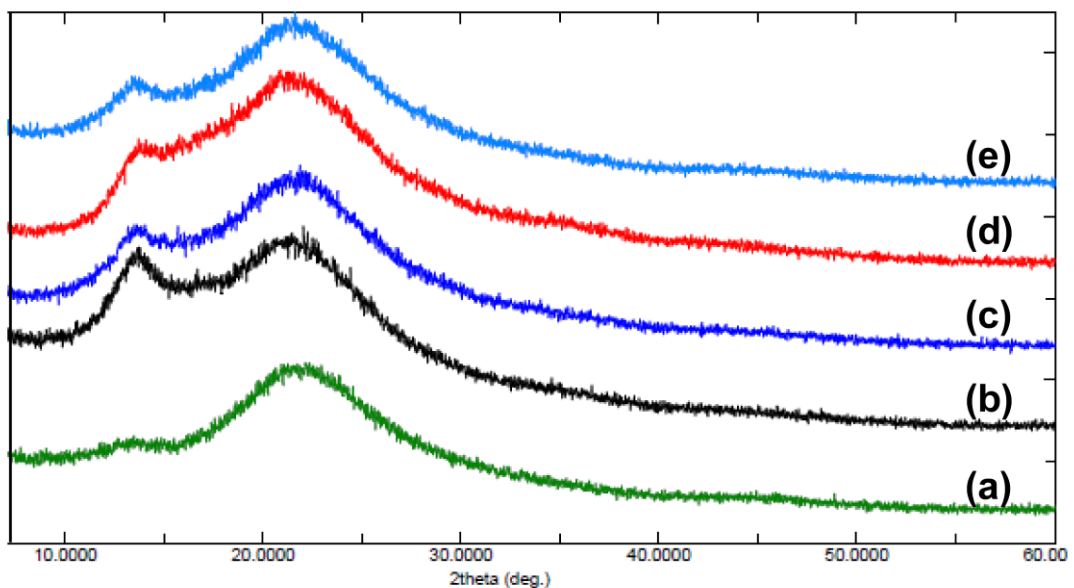


Figure 13: XRD diffractograms of a) NaAlg film, b) PEC-2, c) PEC-3, d) PEC-4 and e) PEC-5 multilayer films

### 3.5 Thermal Gravimetric Analysis (TGA) of the Films

The TGA curves of P<sub>4</sub>VP, Na-Alg, PEC-2, PEC-3, PEC-4 and PEC-5 multilayers are given in Figure 14 a, b, c, d, e, and f respectively. All samples were heated from 25–600 °C with the same heating rate, 10 °C/min. They all show water loss causing 5–15% weight loss up to 120 °C. Figure 14 a shows that P<sub>4</sub>VP exhibits three steps of weight loss. The first step is due to water loss up to 120 °C. The stage within 120–220 °C is related to the thermal process involving the breakdown of the ionic interaction between the protonated P<sub>4</sub>VP and the negatively charged chloride ion. The thermal degradation within 220–350 °C is assigned to the degradation of P<sub>4</sub>VP structure. All of the P<sub>4</sub>VP film degrades at 640 °C. The main weight loss by sodium alginate as shown in Figure 14 b occurs at about 220 °C due to the degradation of the chain backbone. The weight loss that follows within 270–600 °C is due to the degradation of products formed during the first stage. About 40% of the initial weight of the Na-Alg film sample remains at 600 °C. As can be followed from Figure 14 c, d, e and f the TGA curves of the PEC multilayer films are similar to that of sodium alginate, the substrate and the main component of the PEC films. They show two steps of weight loss with a main degradation temperature at around 260°C. When comparing with the sodium alginate, it is observed that the thermal stability of the PEC multilayer films are less than that of the Na-Alg but better than that of P<sub>4</sub>VP with 70% weight loss at the end of the thermal treatment. The onset of degradation, however, occurs at a lower temperature for the PEC multilayer films compared to the parent polymers as shown in Table 4. Na-Alg starts to degrade at 220 °C. It can be followed from Table 4 that Na-Alg has the highest temperature of onset of degradation, and PEC-2 has the lowest, in accordance with their crystallinity index values. Lower crystallinity of PEC-2 results in lower thermal stability. PEC-3, PEC-4

and PEC-5 start degrading at similar temperatures in the temperature range 195-200° C, as they all have comparable crystallinity index values. This observation indicates that during complex formation hydrogen bonding interactions between the alginate chains are disrupted causing some loss in thermal stability as confirmed by XRD analysis.

Table 4: The temperature stages of degradation, weight % and the crystallinity indexes of Na-Alg, PEC-2, PEC-3, PEC-4 and PEC-5

<b>Sample</b>	<b>Crystallinity Index</b>	<b>Stage 1(onset degradation)</b>	<b>Weight % after stage 1</b>	<b>Stage 2</b>	<b>Weight % after stage 2</b>
<b>Na-Alg</b>	0.49	215 °C	80 %	260-600 °C	35 %
<b>PEC-2</b>	0.25	180 °C	88 %	269-600 °C	25 %
<b>PEC-3</b>	0.36	195 °C	88 %	252-600 °C	27 %
<b>PEC-4</b>	0.42	195 °C	82 %	269-600 °C	24 %
<b>PEC-5</b>	0.39	200 °C	85 %	300-600 °C	30 %

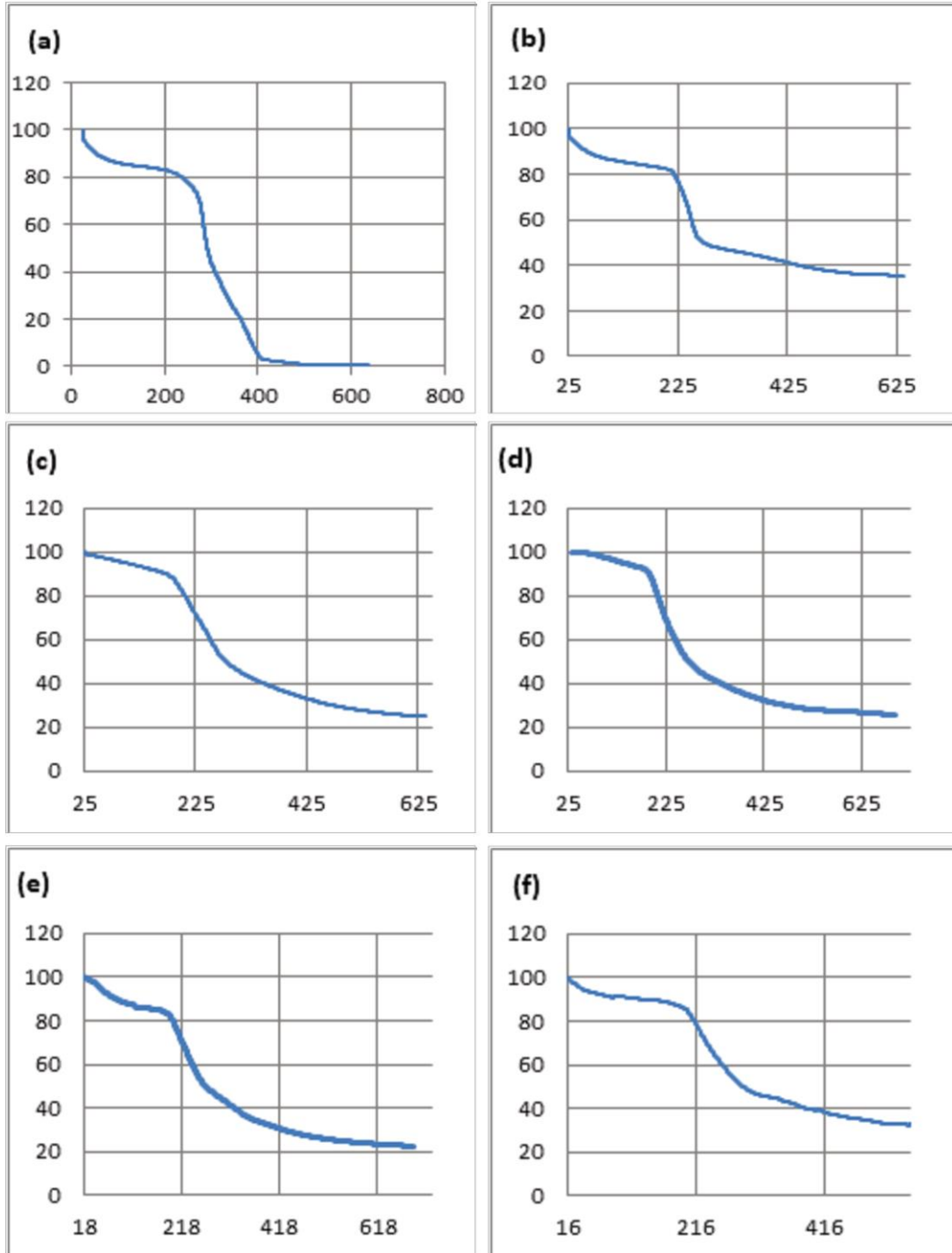


Figure 14: TGA curves for a) P<sub>4</sub>VP b) Na-Alg c) PEC-2 d) PEC-3 e) PEC-4 f) PEC-5

### 3.6 Scanning Electron Microscopy (SEM)

The SEM pictures of Na-Alg, PEC-2, PEC-3, PEC-4 and PEC-5 are given in Figure 15 a, b, c, d and e respectively. Na-Alg exhibits a rough surface with nonporous and heterogeneous morphology due to some insoluble alginate particles adhering on the



surface of the film [97]. A similar observation can be made for PEC-3 and PEC-5 whose outer surfaces are Na-Alg. The surfaces of the films with P<sub>4</sub>VP outer layer, PEC-2 and PEC-4, are smoother compared to the others, with polymer particles adhered on the film surface. The film surfaces contain some cracks due to the stress created during solvent evaporation. The surface roughness was further analyzed by AFM.

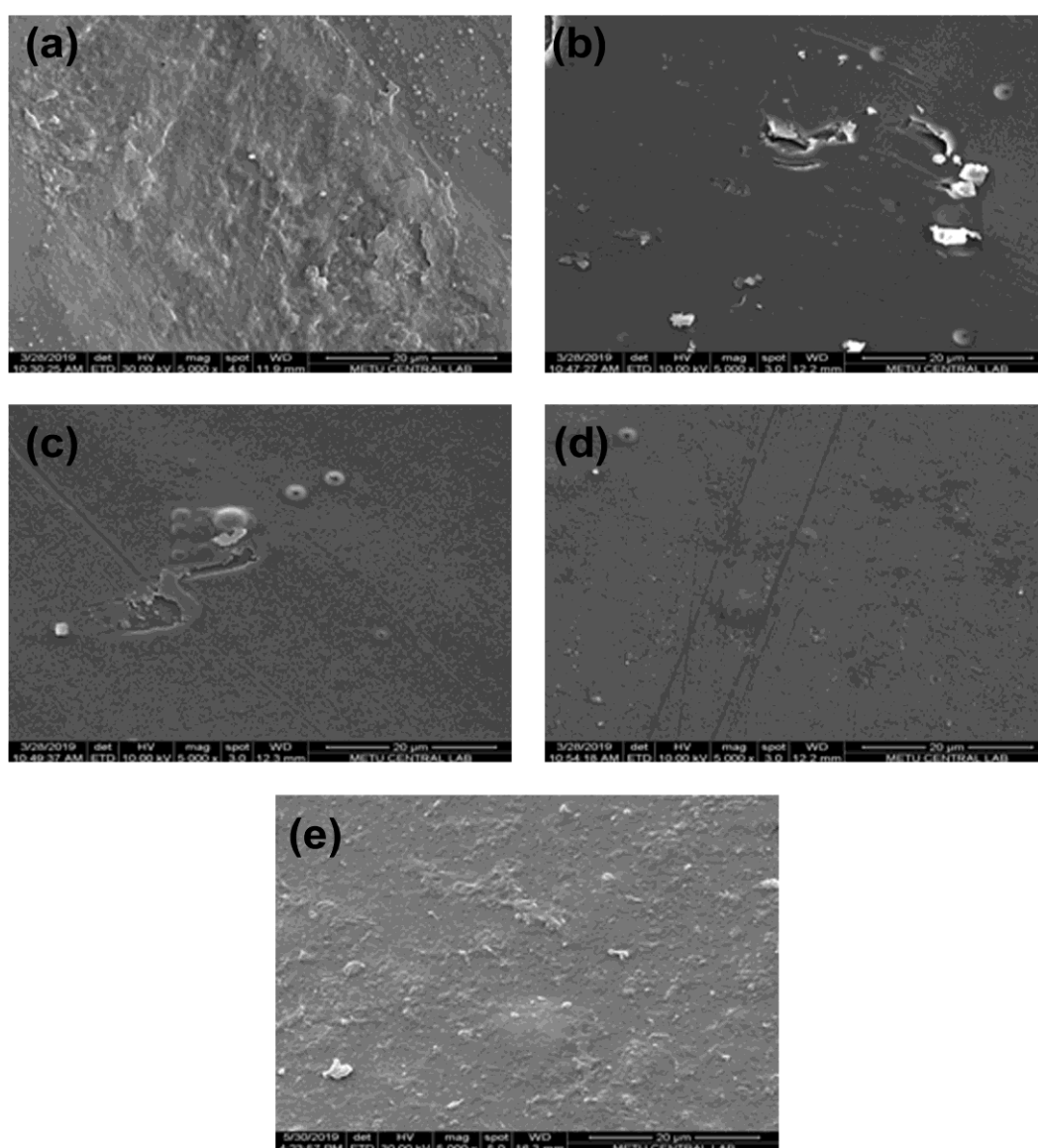


Figure 15: SEM micrographs of a) Na-Alg, b) PEC-2 c) PEC-3 d) PEC-4 and e) PEC-5 multilayer films (5000x magnification)

### 3.7 Atomic Force Microscopy (AFM) and Contact Angle (CA)

AFM analysis was done in order to give details about surface morphology and roughness for Na-Alg and the different PEC multilayer membranes. Figure 16 (left column) shows surface morphologies and the corresponding roughness parameter, root mean square of roughness ( $R_q$ ), of the films. The contact angle, CA values are given in Figure 16 (right column). Generally, the topographic features of the membranes change significantly by adding either Na-Alg or P<sub>4</sub>VP as new layers onto the main substrate. Three factors affect the topology of the films. These are the nature of the polymer forming the outer layer, the crystallinity index and the number of layers. The main factor that affects the topology is the nature of the polymer forming the outer layer. Na-Alg, PEC-3 and PEC-5 in Figure 16 (a), (c) and (e) respectively show similar topographic features as they all have the alginate as the outer layer. Parallel to what is observed with films having alginate outer layers, topologies of PEC-2 and PEC-4 in Figure 16 (b) and (d) respectively resemble each other due to the characteristic feature of the outer layer, P<sub>4</sub>VP. The surface roughness of the pure Na-Alg is represented by an  $R_q$  value of 4.02 nm. Bright prominent parts are attributed to self-aggregation of Na-Alg chains [97]. The Na-Alg film bears the highest crystallinity index of 0.49, and the lowest  $R_q$  value among the samples studied. On the surface of PEC-2, P<sub>4</sub>VP chains, which form a diffuse layer on the Na-Alg substrate, are observed as bright domains. The  $R_q$  value increases to 27.9 nm indicating increased roughness of the surface. This sample has the lowest crystallinity index with 0.25, and the highest  $R_q$  value. Examining the AFM image of PEC-3 reveals circular, self-aggregated Na-Alg outer layer as bright domains. Interestingly, the  $R_q$  value decreases to 16.3 nm showing that a smoother surface is achieved when PEC-3 is formed. This must be due to the nature of alginate chains,

which align on the surface. The sample has a crystallinity index of 0.36, which is lower than that of the Na-Alg film but higher than that of PEC-2. Adding a fourth layer, which is P<sub>4</sub>VP, on top of PEC-3, causes an increase in the surface roughness to 23.2 nm. PEC-4 surface exhibits more diffuse domains of P<sub>4</sub>VP chains as the outer layer. The decrease from 27.4 nm to 23.2 nm from PEC-2 to PEC-4 should be due to higher crystallinity index (0.42) compared to PEC-2 (0.25). The last film, PEC-5 has a surface morphology similar to that of PEC-3 due to the alginate outer layer. The Rq value decreases compared to PEC-4 revealing the contribution of alginate alignment to surface morphology. PEC-5 with a crystallinity index of 0.39 has a higher Rq (20.2 nm) value compared to PEC-3 (16.3 nm) as the number of layers is higher.

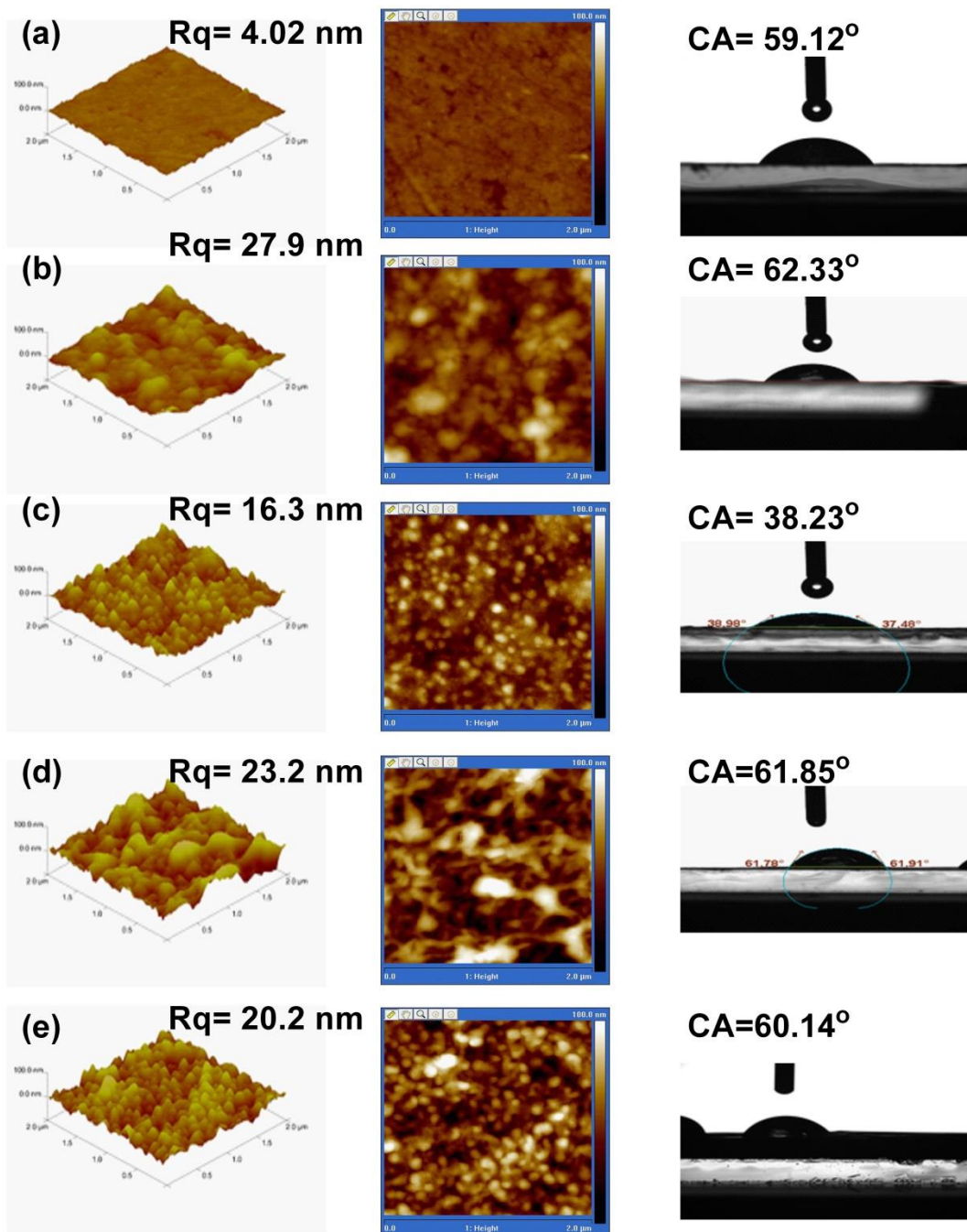


Figure 16: AFM analysis (left and middle column) and contact angles (right column) of water droplets of a) NaAlg, b) PEC-2, c) PEC-3, d) PEC-4 and e) PEC-5

The contact angle (CA) values show a similar trend as observed with surface roughness, Rq values. Na-Alg film, PEC-2, PEC-4 and PEC-5 have similar contact angle values given as 59.2°, 62.3°, 61.8° and 60.14° as shown in Figure 17 exhibiting moderately hydrophilic surfaces. PEC-3, on the other hand, demonstrates a

significantly lower contact angle value with  $38.2^\circ$  as shown in Figure 17. PEC-3 surface is much more hydrophilic than those of the others. This sample has the lowest roughness among all. Hence, it can be deduced that there is a correlation between surface roughness and CA values as explained by Wenzel in 1936 [98]. It is well known that "adding surface roughness will add to wettability caused by the chemistry of the surface". Higher roughness results in higher CA values. Furthermore, free carboxylic acid groups available on PEC-3 surface should contribute to increased H-bonding interaction with water, making the surface more hydrophilic.

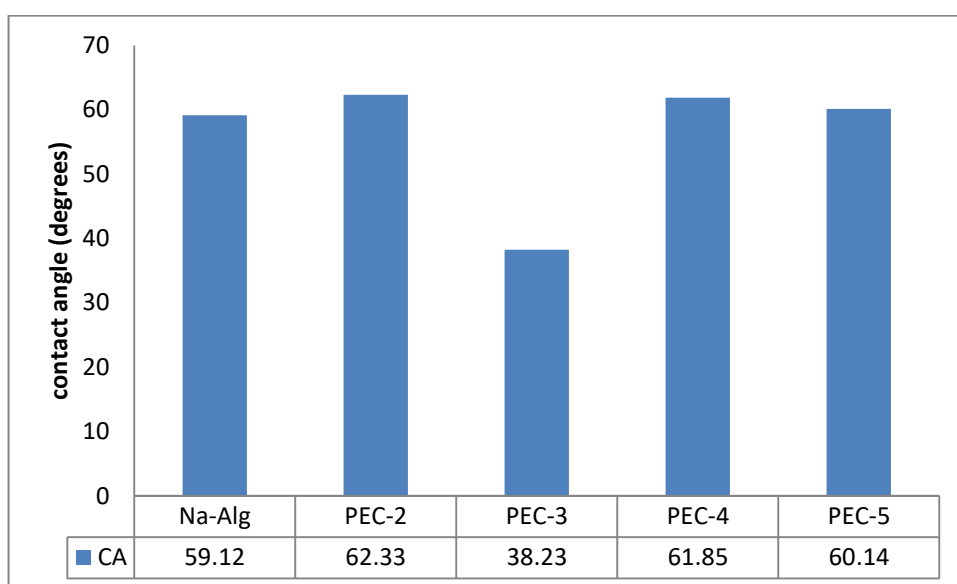


Figure 17: Contact angles of Na-Alg and the PEC multilayer membranes

### 3.8 Solubility of PEC Multilayer Films

The PEC multilayers have been immersed in different solvents as shown in Table 5. The PEC multilayers are insoluble in all of the organic solvents (polar and nonpolar) but swells in water and in acid buffer solution at pH=1.2. At pH values 4.2 and above the PEC disintegrates due to the fact that increasing pH will deprotonate the nitrogen atom in the P<sub>4</sub>VP, and this will break down the PEC.

Table 5: Solubility behavior of the PEC multilayers in different solvents

Solvent	Result
H <sub>2</sub> O	Swell
Ethanol	Insoluble
HCl (1M)	Swell
pH=7.4 (buffer)	dissolve
pH=1.2 (buffer)	swell
pH=4.2 (buffer)	dissolve
DMSO	Insoluble
DMF	Insoluble
Toluene	Insoluble
CHCl <sub>3</sub>	Insoluble
Acetone	Insoluble

### 3.9 Swelling

Figure 18(a) and (b) show the swelling behavior of PEC-2, PEC-3, PEC-4 and PEC-5 in water and HCl buffer solution (pH= 1.2) respectively. All samples swell rapidly both in distilled water and in pH=1.2 buffer solution. They all reach equilibrium within five minutes since these thin films with an average thickness of 0.011 mm. The % swelling results in water for PEC-2, PEC-3, PEC-4 and PEC-5 shown in Figure 18(a) are 85%, 135%, 90% and 215% respectively. While in Figure 18(b) gives the % swelling in acid buffer of 95%, 130%, 65% and 155% for PEC-2, PEC-3, PEC-4 and PEC-5 respectively.

The % swelling of PEC-2 and PEC-4 with the same outer layer (P<sub>4</sub>VP), PEC-2 swells more than PEC-4 due to its more amorphous nature allowing diffusion of water molecules easily, also PEC-2 swells more in acid than PEC-4 since due to the lower crystallinity of PEC-2 than PEC-4.

While, for PEC-3 and PEC-5 with the Na-Alg as the outer layer; PEC-5 has an equilibrium swelling capacity higher than that of PEC-3 due to the higher roughness of PEC-5 allowing easier diffusion of water molecules.

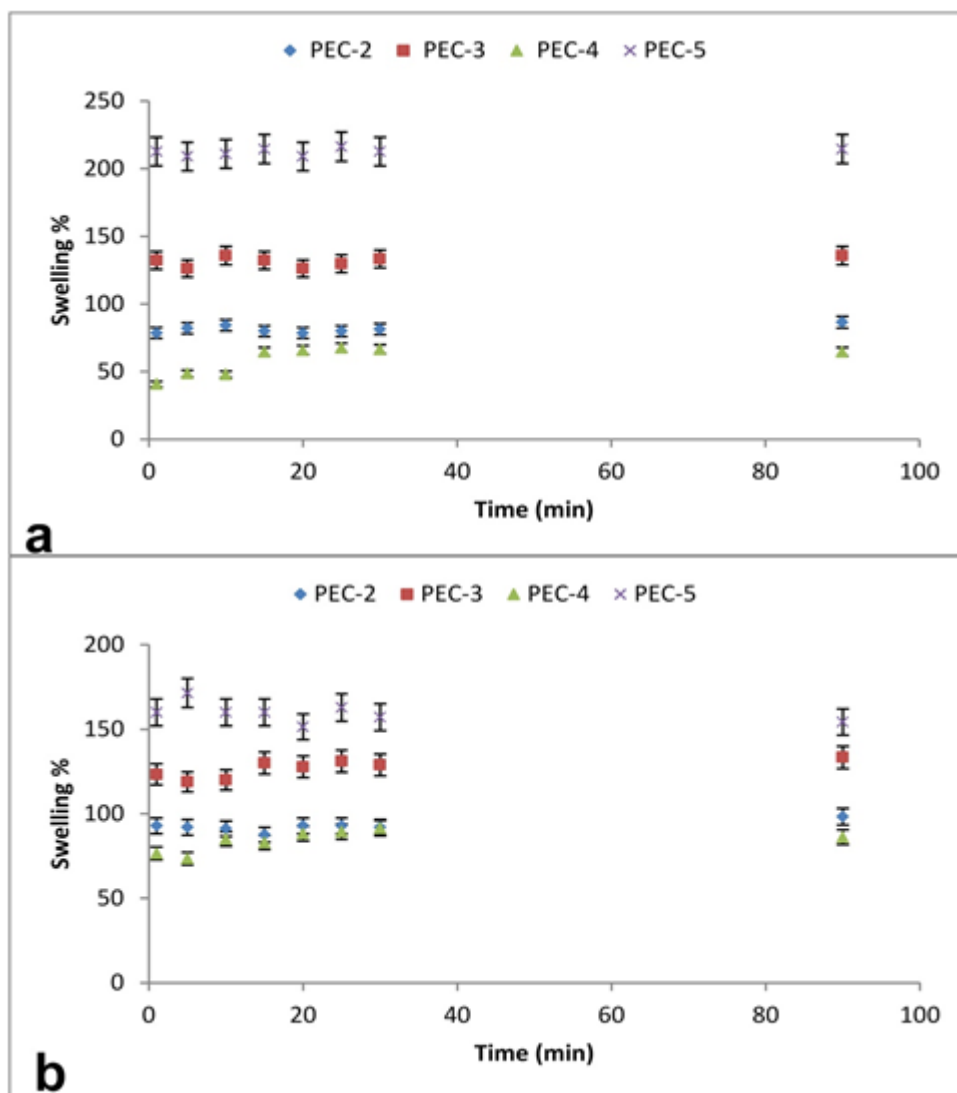


Figure 18: Swelling % for polyelectrolyte multilayers PEC-2, PEC-3, PEC-4 and PEC-5 in a) water and in b) acidic buffer

### 3.10 Drug Loading and Release

#### 3.10.1 Drug Loading

CIP.HCl was loaded on the PEC multilayer films by immersing them in the drug solution. Table 6 shows the effect of immersing time of the films on the loading

efficiency in 12.5 ppm solution. The best time for loading of the membranes in the drug solution is two days and also it shows that PEC-3 has the highest % loading efficiency among all of the PEC multilayer films. The drug loading efficiency and drug loading capacity for the PEC multilayers in 12.5 ppm and 20.0 ppm initial drug concentrations are summarized in Table 7. The drug loading capacity/efficiency and drug release were evaluated according to the calibration curve of the drug CIP.HCl as shown in Figure 19.

Table 6: Effect of loading time on the loading efficiency on the different PEC multilayer films at 12.5 ppm concentration

loading time (day)	PEC-2	PEC-3	PEC-4	PEC-5
1	75.16	33.39	63.28	55.45
2	74.62	88.87	78.53	74.24
3	71.25	87.03	71.02	73.1
4	73.54	87.42	75.08	74.25
5	69.10	87.65	68.42	72.36

Table 7: Drug loading capacity and drug loading efficiency of the different PEC multilayers

Multilayer sample	Drug loading efficiency		Drug loading capacity	
	12.5 ppm	20 ppm	12.5 ppm	20 ppm
PEC-2	74.62 %	45.22 %	3.09 %	2.38 %
PEC-3	88.87 %	66.71 %	3.51 %	3.51 %
PEC-4	78.53 %	46.81 %	2.88 %	2.47 %
PEC-5	74.24 %	64.32 %	2.86 %	3.39 %



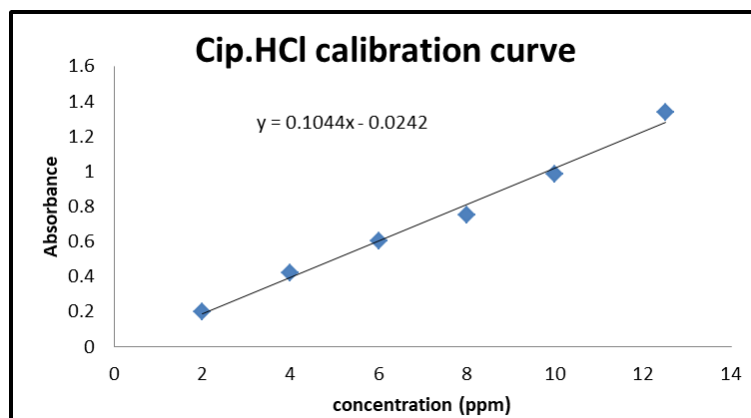


Figure 19: Calibration curve for CIP.HCl solution

Both drug loading capacity and drug loading efficiency values of PEC-3 are higher than those of the others. This behavior can be attributed to higher hydrophilicity of PEC-3 allowing better diffusibility of the drug into the membrane structure. Drug loading capacities of PEC-2 and PEC-4 films are higher in 12.5 ppm than in 20.0 ppm CIP.HCl solution. However, PEC-3 has the same loading capacity both in 12.5 and 20.0 ppm solutions and PEC-5 reaches that of PEC-3 in 20.0 ppm solution. These results indicate that hydrophilicity of the outer layer is critical in determining the degree of polymer-drug interactions. Higher hydrophilicity results in higher loading capacities.

Figure 19 shows SEM photos for the CIP.HCl loaded PEC multilayers. It is clearly seen from Figure 21(a) that the drug is mainly loaded on the outer portion of the multilayer membrane, PEC-2, while there is a relatively much smaller amount of drug observed on the outer portion of PEC-3 as in Figure 20(b), indicating that a greater portion of CIP.HCl diffuses into the inner layers of PEC-3. The fact that the drug adheres on the outer layers shows good compatibility between the drug and the membrane surface. The fact that PEC-3 contains less amount of drug on the outer surface accounts for the higher loading capacity of PEC-3.

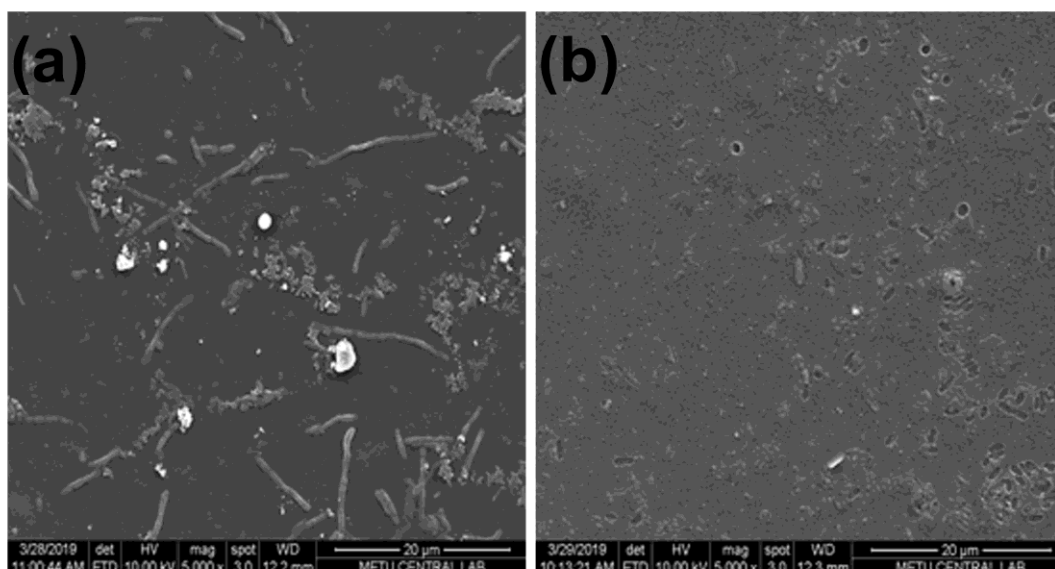


Figure 20: SEM pictures for the CIP.HCl loaded multilayers a) in PEC-2 and b) in PEC-3

### 3.10.2 In vitro CIP.HCl Release from NaAlg/P<sub>4</sub>VP PEC Films

The release of CIP.HCl has been carried out in water and in pH=1.2 HCl/KCl buffer solution at 37 °C for the different PEC multilayer membranes, PEC-2, PEC-3, PEC-4 and PEC-5. Figures 21 and 22 show the cumulative drug release profiles of the PEC multilayer films in both water and in acidic medium for the loaded samples in two different concentrations 12.5 and 20.0 ppm for 120 minutes release time respectively. It can be observed that there is a burst release effect within 30 minutes, which is more pronounced in acidic medium due to higher solubility of the drug in acid solution and due to breaking down the intermolecular hydrogen bonds formed during the formation of the films [99]. It can be clearly seen that all PEC multilayer membranes studied, released the drug in acidic medium faster than in water for both initial drug concentrations. Furthermore, almost the entire drug loaded is released in acidic medium after one day with 99.7%, 99.4%, 99.3% and 99.7% for PEC-2, PEC-3, PEC-4 and PEC-5 respectively for 20.0 ppm initial drug concentration. The corresponding values for 12.5 ppm initial drug concentration are 91.5%, 91.9%,

98.9% and 97.9% respectively. When the release medium is water, on the other hand, the cumulative % release values are much lower. The cumulative % release values are 47.4%, 29.2%, 46.4% and 32.0% at 20.0 ppm drug solution for PEC-2, PEC-3, PEC-4 and PEC-5 respectively. For the 12.5 ppm drug solution, these values are 58.3%, 65.3%, 55.3% and 67.6% respectively. It is interesting to note that even though the amount of drug loaded in PEC-3 is not affected by the initial concentration of the drug in the loading medium, less amount of drug is released when the initial concentration of the drug in the loading medium is higher. Similarly, no matter the loading capacity, the cumulative % release is less for 20.0 ppm initial concentration for all other PEC films studied as well. This behavior can be explained by the distribution of the drug within the polymer matrix. It is anticipated that during loading the drug molecules initially interact with the outer layers of the PEC film. Hence, at low concentrations the drug molecules are mostly found at the outer layers and diffuse out faster. At higher concentrations, however, drug molecules diffuse into the inner layers after reaching equilibrium concentration on the outer layers. Hence, cumulative drug release is less within the same period of time. When the results are examined according to the arrangement of the layers, it can be observed that PEC-2 and PEC-4 with P<sub>4</sub>VP as the outer layer show lower % release values after one day with 58.3% and 55.3% respectively compared to PEC-3 and PEC-5 whose the outer layer is Na-Alg. These films have 65.3% and 67.6% for PEC-3 and PEC-5 respectively as shown in Table 8. Similarly for 12.5 ppm drug solution set, the cumulative % release values for PEC-2 and PEC-4 are comparable as well as for PEC-3 and PEC-5 pair. Generally, the fast release in both media means some fraction of the drug is loaded in the outer portion of the multilayer membranes' surfaces so

that the drug diffuses faster. Also, the solubility of the drug plays an important role in determining if the release is fast or slow [100].

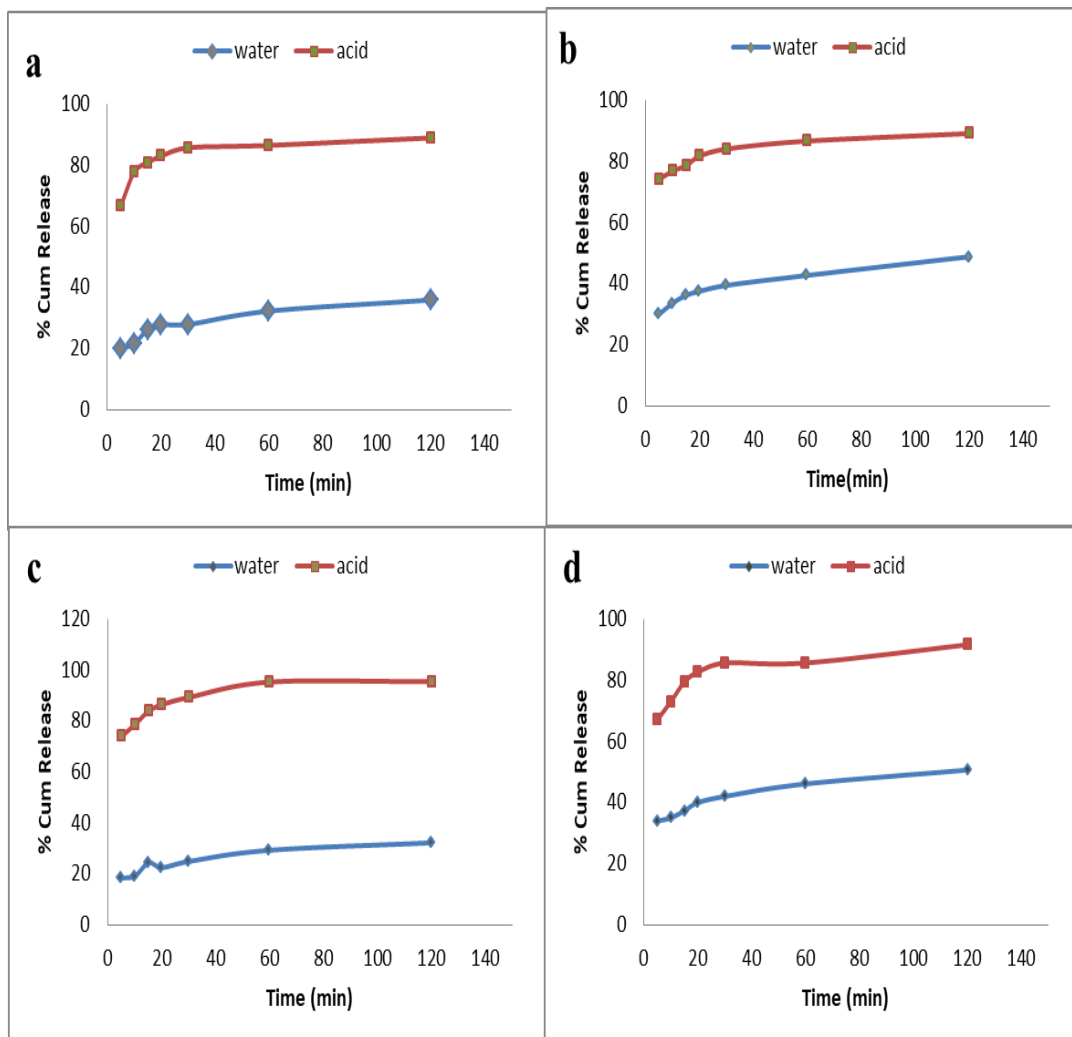


Figure 21: The % cumulative release for a) PEC-2, b) PEC-3, c) PEC-3 and d) PEC-5 in both water and in pH=1.2 buffer solution for 12.5 ppm drug solution

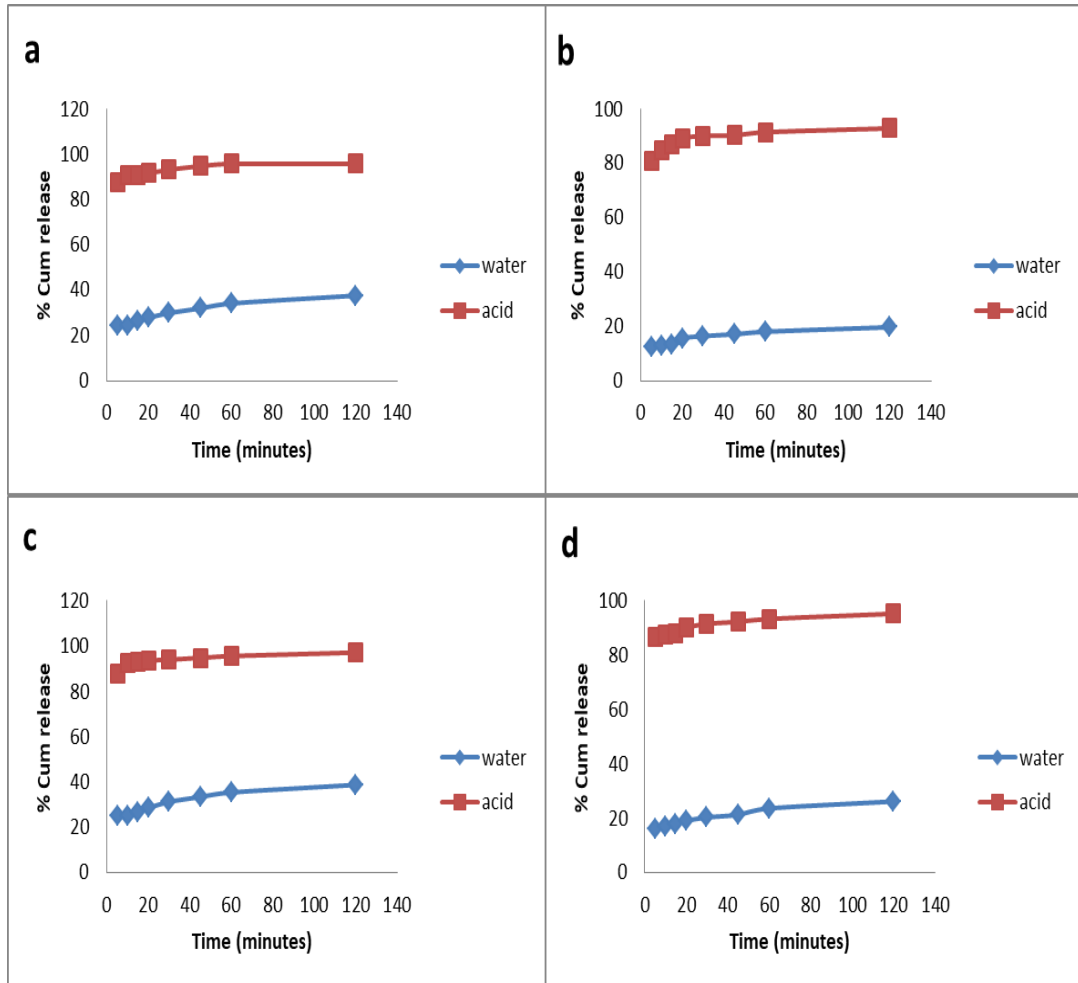


Figure 22: The % cumulative release for a) PEC-2, b) PEC-3, c) PEC-3 and d) PEC-5 in both water and in pH=1.2 buffer solution for 20 ppm drug solution

Table 8: Cumulative % release values after one day for all PEC samples at 20 and 12.5 ppm concentrations

<b>Cumulative % release for 20.0 ppm drug solution</b>		
<b>PEC film</b>	<b>In acidic solution</b>	<b>In H<sub>2</sub>O</b>
<b>PEC-2</b>	99.7	47.4
<b>PEC-3</b>	99.4	29.2
<b>PEC-4</b>	99.3	46.4
<b>PEC-5</b>	99.7	32.0
<b>Cumulative % release for 12.5 ppm drug solution</b>		
<b>PEC film</b>	<b>In acidic solution</b>	<b>In H<sub>2</sub>O</b>
<b>PEC-2</b>	91.5	58.3
<b>PEC-3</b>	91.9	65.3
<b>PEC-4</b>	98.9	55.3
<b>PEC-5</b>	97.9	67.6

### 3.10.3 Drug Release Kinetics

Different mathematical models were used to determine the behavior of the release in the multilayer films in both water and acidic buffer solution with pH=1.2 for the two different concentrations 12.5 and 20.0 ppm. The correlation coefficient ( $R^2$ ) values were calculated as shown in Table 9 according to zero order, first order, Higuchi and Korsmeyer-Peppas models. Comparing the  $R^2$  values in Table 9, all the release kinetics of the PEC multilayer films follow Higuchi's model better than other models in both water and acidic buffer considering higher values of  $R^2$ . Release kinetics are shown in Figures 23-30 indicating that CIP.HCl release from the PEC films studied, follow Higuchi's model in water and even though release kinetics in acid buffer (pH=1.2) follow Higuchi's model better than zero order or first order release kinetics, the behavior in acid buffer does not obey Higuchi's model as good as in water.

Higuchi's model is developed to study the release of water soluble drugs incorporated in solid matrix [101]. The PEC films used in this study can be taken as examples to diffusion controlled drug delivery system, which is a matrix system that contains drug dispersed in the medium. The system overall is a monolithic dispersion [50]. In such systems, Higuchi's model of drug release is applicable and the data presented below indicates drug release behavior obeys Higuchi's model. The assumption made by Higuchi when studying the release of the drug from thin film into the skin is as follows [102]:

- (1) Chemical, physical and environmental conditions can limit the transportation of the drug through the films, while through the skin the transportation is rapid.
- (2) The concentration of the drug in the skin is assumed to be negligible.
- (3) The drug dispersed smoothly into the film due to its thickness, which it is greater than the particle size of the drug.

- (4) The drug is distributed homogeneously over the film.
- (5) The dissolved drug particles diffuse through the film is slower comparing to its dissolution within the film.
- (6) Neither time nor the position of the drug within the film can affect the constant the "diffusion coefficient".
- (7) During the release of the drug, the film will not dissolve or swell.

In the data presented in Table 9, it can be observed that  $K_H$  values of the different films do not show a trend with respect to the identity of the outer layer or the number of layers because  $K_H$  contains for different variables (equation 9), some of which such as  $C_s$  and  $D$  cannot be measured directly. Also some  $R^2$  values in acidic medium are below 0.90 due the burst effect operating during the initial stages of drug release. Furthermore, Higuchi equations deviate from ideality and do not pass through the origin again due to the strong burst effect. Also, the films swell in aqueous medium. Hence the system does not obey postulate (7) in the original Higuchi postulate. Moreover, other postulates may not be obeyed perfectly either.

Korsmeyer-Peppas model is used for the analysis of the mechanism of the released drug, depending on the  $n$  values shown in Table 9. The release mechanism of the system could be described as Fickian diffusion mechanism since all the values are less than 0.5.

Table 9: In vitro dissolution kinetics of ciprofloxacin HCl in 20 and 12.5 ppm in all films

20 ppm H <sub>2</sub> O						
	Zero order	First order	Higuchi		Korsmeyer-Peppas	
PEC films	R <sup>2</sup>	R <sup>2</sup>	R <sup>2</sup>	K <sub>H</sub>	R <sup>2</sup>	n
PEC-2	0.90	0.91	0.99	2.06	0.96	0.1349
PEC-3	0.80	0.81	0.91	1.32	0.98	0.1610
PEC-4	0.88	0.89	0.99	2.24	0.97	0.1597
PEC-5	0.91	0.92	0.98	1.40	0.92	0.1467
20 ppm acid						
	Zero order	First order	Higuchi		Korsmeyer-Peppas	
PEC films	R <sup>2</sup>	R <sup>2</sup>	R <sup>2</sup>	K <sub>H</sub>	R <sup>2</sup>	n
PEC-2	0.65	0.73	0.98	1.23	0.96	0.0296
PEC-3	0.60	0.72	0.82	1.28	0.93	0.0402
PEC-4	0.63	0.72	0.82	1.28	0.86	0.0201
PEC-5	0.82	0.92	0.94	1.29	0.98	0.0342
12.5 ppm H <sub>2</sub> O						
	Zero order	First order	Higuchi		Korsmeyer-Peppas	
PEC films	R <sup>2</sup>	R <sup>2</sup>	R <sup>2</sup>	K <sub>H</sub>	R <sup>2</sup>	n
PEC-2	0.82	0.82	0.86	1.99	0.98	0.240
PEC-3	0.78	0.78	0.97	1.89	0.98	0.179
PEC-4	0.85	0.85	0.85	1.91	0.95	0.261
PEC-5	0.85	0.85	0.96	2.37	0.95	0.191
12.5 ppm acid						
	Zero order	First order	Higuchi		Korsmeyer-Peppas	
PEC films	R <sup>2</sup>	R <sup>2</sup>	R <sup>2</sup>	K <sub>H</sub>	R <sup>2</sup>	n
PEC-2	0.48	0.70	0.80	1.80	0.90	0.107
PEC-3	0.76	0.84	0.92	2.13	0.98	0.076
PEC-4	0.66	0.89	0.95	2.39	0.99	0.109
PEC-5	0.63	0.54	0.66	2.42	0.99	0.120



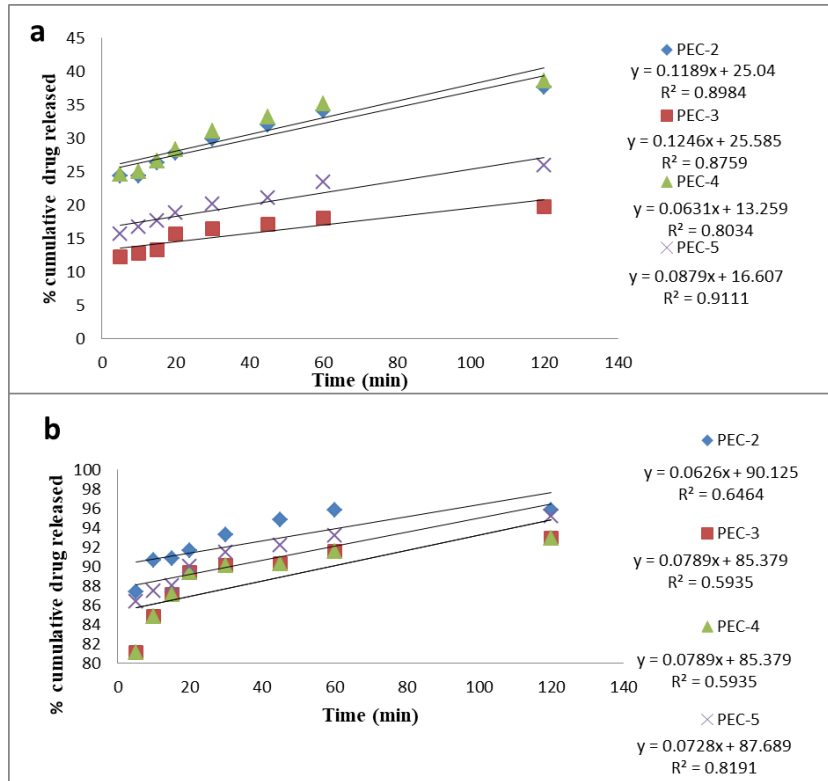


Figure 23: Zero order kinetics for the release of CIP.HCL from the 20 ppm loaded PEC films in a) water and in b) acid buffer pH=1.2

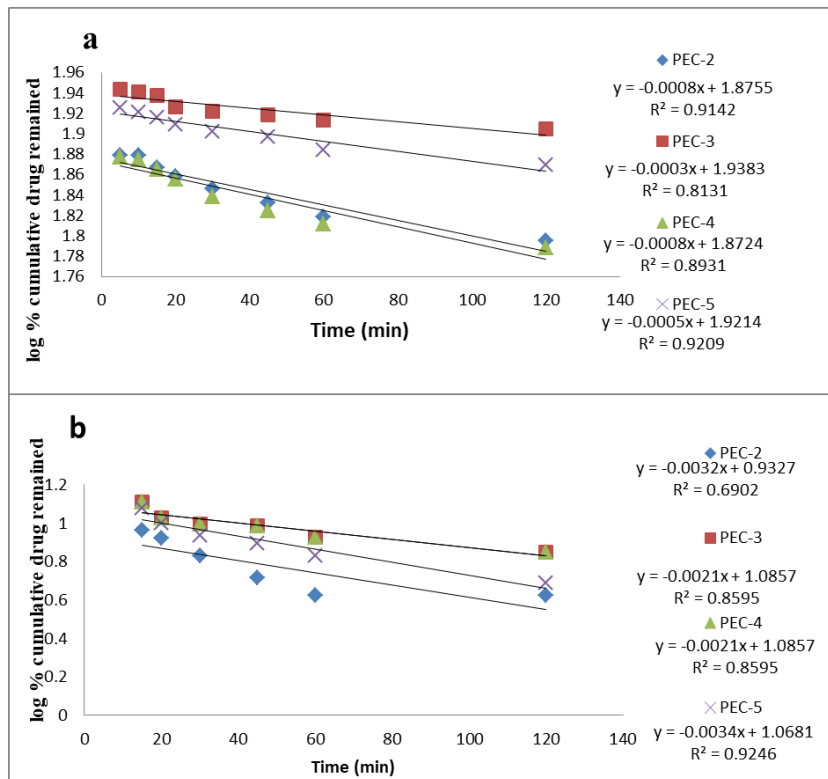


Figure 24: First order kinetics for the release of CIP.HCL from the 20 ppm loaded PEC films in a) water and in b) acid buffer pH=1.2

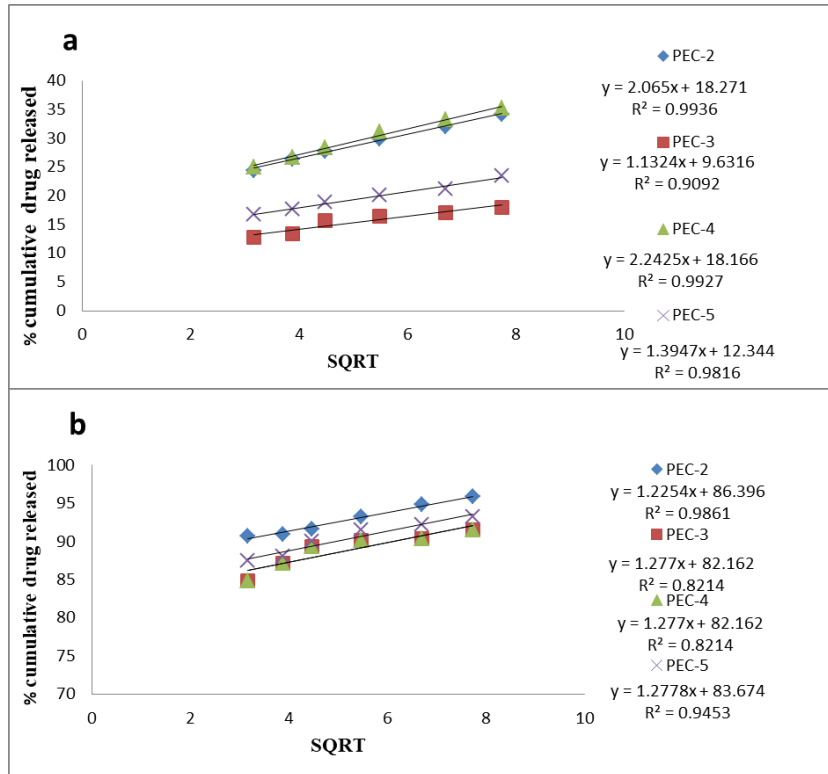


Figure 25: Higuchi kinetics for the release of CIP.HCL from the 20 ppm loaded PEC films in a) water and in b) acid buffer pH=1.2

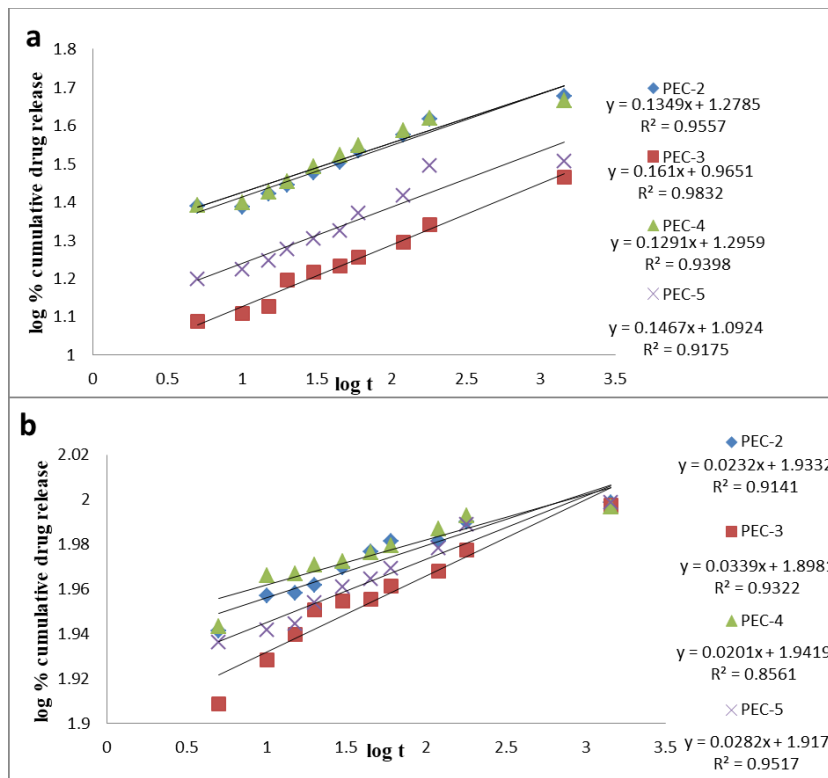


Figure 26: Korsmeyer-Peppas kinetics for the release of CIP.HCL from the 20 ppm loaded PEC films in a) water and in b) acid buffer pH=1.2

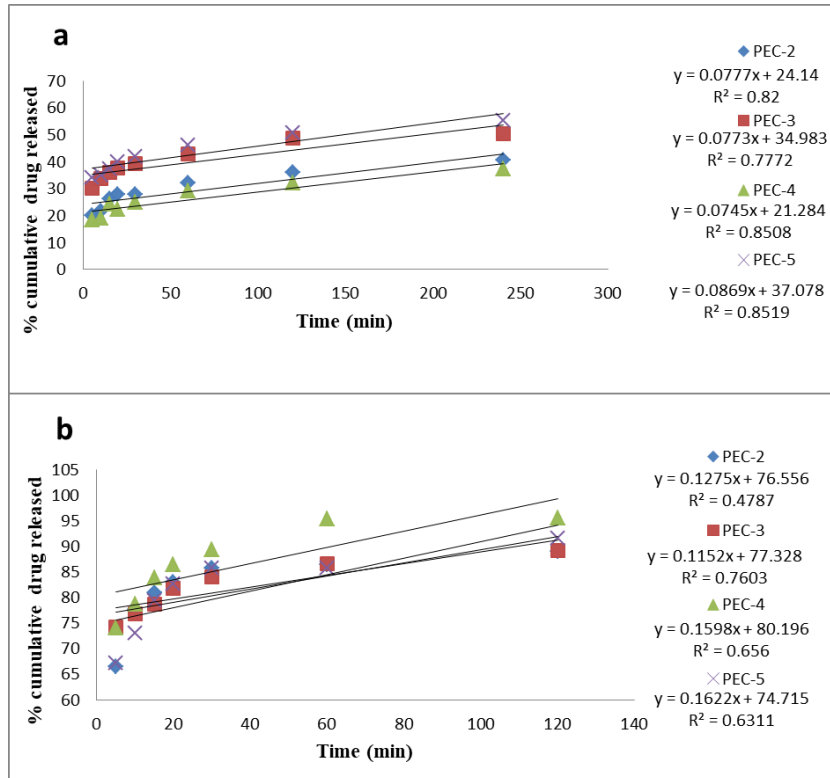


Figure 27: Zero order kinetics for the release of CIP.HCL from the 12.5 ppm loaded PEC films in a) water and in b) acid buffer pH=1.2

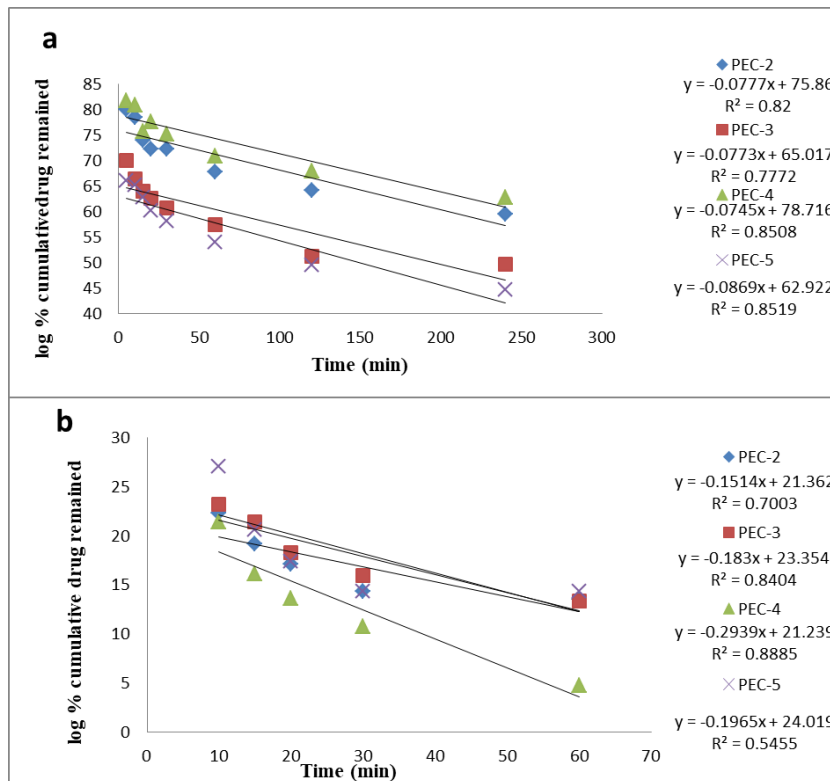


Figure 28: First order kinetics for the release of CIP.HCL from the 12.5 ppm loaded PEC films in a) water and in b) acid buffer pH=1.2

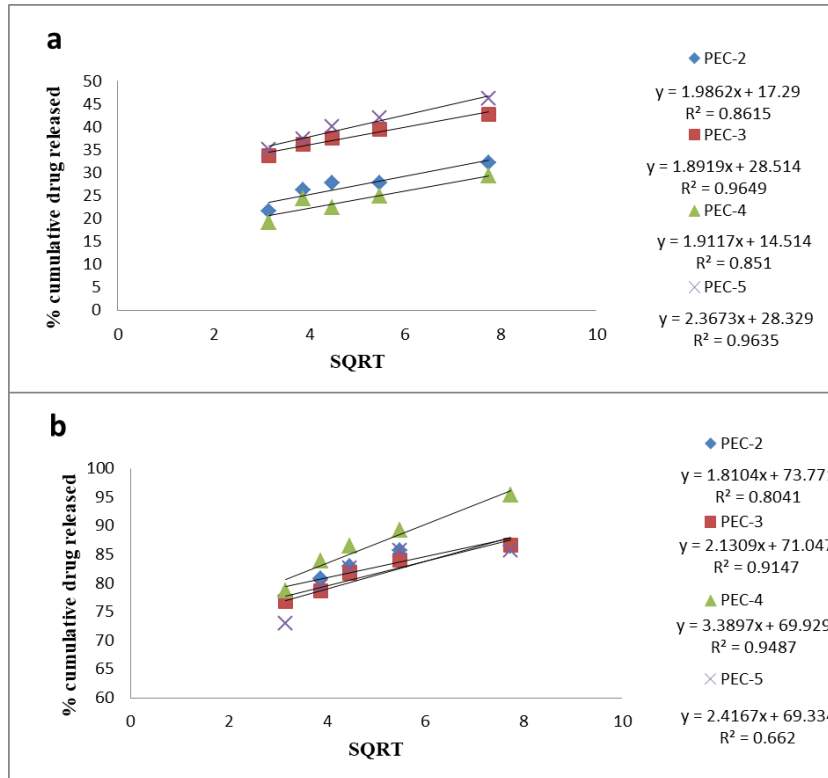


Figure 29: Higuchi kinetics for the release of CIP.HCL from the 12.5 ppm loaded PEC films in a) water and in b) acid buffer pH=1.2

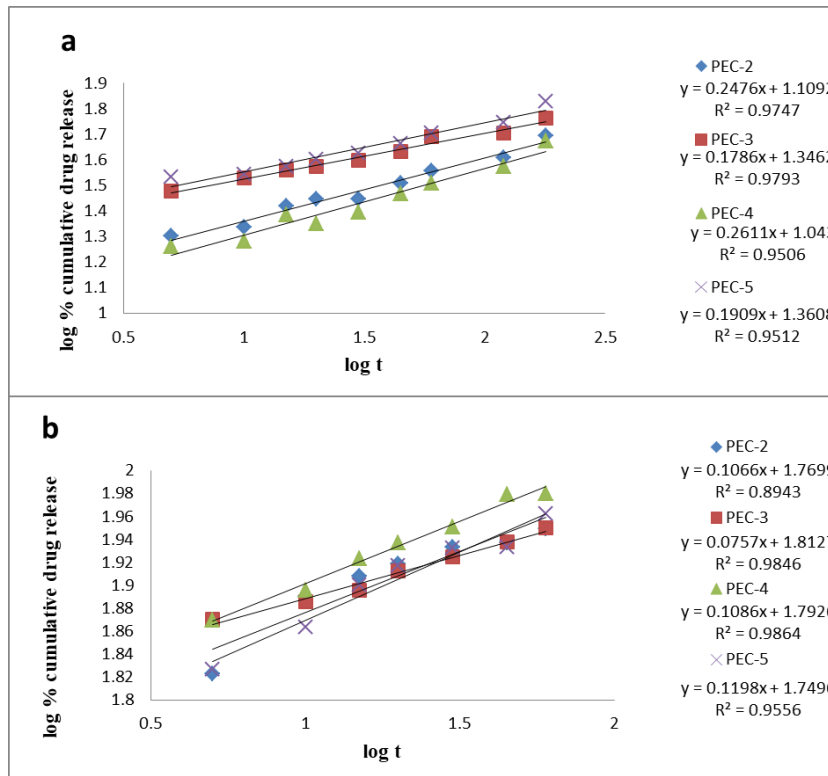


Figure 30: Korsmeyer-Peppas kinetics for the release of CIP.HCL from the 12.5 ppm loaded PEC films in a) water and in b) acid buffer pH=1.2

## Chapter 4

### CONCLUSION

In the present work Na-Alg/P<sub>4</sub>VP polyelectrolyte complex multilayer films were successfully prepared through immersing process. The number of layers and the nature of the outer layer affect the physicochemical properties of the films. The multilayer Na-Alg/P<sub>4</sub>VP films prepared are thin, transparent, hydrophilic matrices stable in acidic buffer up to pH 4.2. Their solubility and swelling characteristics indicate that these films could act as potential transdermal drug delivery systems for skin wound healing under acidic conditions. The films prepared proved to be suitable matrices for loading and release of the antibacterial agent ciprofloxacin HCl. The three layer film PEC-3, which is composed of Na-Alg/P<sub>4</sub>VP/Na-Alg layers is characterized by the lowest roughness, and lowest contact angle among all other multilayer PEC films prepared. It provides a smooth, hydrophilic surface, and optimum swelling capacity, which allows highest drug loading capacity among all others. The drug is well dispersed in the film matrix and is released via diffusion mechanism following  $t^{1/2}$  kinetics. The release mechanism is established as Fickian according to the Korsmeyer-Peppas equation. These results indicate that Na-Alg/P<sub>4</sub>VP films can be considered as suitable matrices for transdermal delivery systems upon further investigations.

## **Chapter 5**

### **FUTURE WORK**

Further modifications are recommended for the development of the films, such as increasing the number of layers and including a third polyelectrolyte in the system other than Na-Alg or P<sub>4</sub>VP with the data obtained in this work. The effect of these new parameters on swelling, thermal stability, crystallinity, hydrophilicity and ciprofloxacin HCl loading/release profile of the films are to be studied. The drug loading method can be modified by including the drug in one of the polymer solutions. Furthermore, new drugs can be tested.

More applications can be tested on these films such as in the environmental field for the removal of organic dyes or heavy metals from wastewater.

## REFERENCES

- [1] V. Siracusa, P. Rocculi, S. Romani, and M. Dalla Rosa, “Biodegradable polymers for food packaging: a review,” *Trends Food Sci. Technol.*, vol. 19, no. 12, pp. 634–643, 2008.
- [2] K. Leja and G. Lewandowicz, “Polymer Biodegradation and Biodegradable Polymers-a Review.,” *Polish J. Environ. Stud.*, vol. 19, no. 2, 2010.
- [3] K. G. Harding, J. S. Dennis, H. Von Blottnitz, and S. T. L. Harrison, “Environmental analysis of plastic production processes: comparing petroleum-based polypropylene and polyethylene with biologically-based poly- $\beta$ -hydroxybutyric acid using life cycle analysis,” *J. Biotechnol.*, vol. 130, no. 1, pp. 57–66, 2007.
- [4] Z. Meng, X. Zheng, K. Tang, J. Liu, and S. Qin, “Dissolution of natural polymers in ionic liquids: A review,” *e-Polymers*, vol. 12, no. 1, 2012.
- [5] G. E. Luckachan and C. K. S. Pillai, “Biodegradable polymers-a review on recent trends and emerging perspectives,” *J. Polym. Environ.*, vol. 19, no. 3, pp. 637–676, 2011.
- [6] A. Aravamudhan, D. M. Ramos, A. A. Nada, and S. G. Kumbar, “Natural polymers: polysaccharides and their derivatives for biomedical applications,” in *Natural and synthetic biomedical polymers*, Elsevier, 2014, pp. 67–89.

- [7] R. Sridhar, R. Lakshminarayanan, K. Madhaiyan, V. A. Barathi, K. H. C. Lim, and S. Ramakrishna, “Electrosprayed nanoparticles and electrospun nanofibers based on natural materials: applications in tissue regeneration, drug delivery and pharmaceuticals,” *Chem. Soc. Rev.*, vol. 44, no. 3, pp. 790–814, 2015.
- [8] A. Sandeep, K. Sangameshwar, G. Mukesh, R. Chandrakant, and D. Avinash, “A brief overview on chitosan applications,” *Indo Am. J. Pharm. Res.*, vol. 3, no. 12, pp. 1564–4574, 2013.
- [9] K. Y. Lee and D. J. Mooney, “Alginate: properties and biomedical applications,” *Prog. Polym. Sci.*, vol. 37, no. 1, pp. 106–126, 2012.
- [10] C. Jeon, J. Y. Park, and Y. J. Yoo, “Novel immobilization of alginic acid for heavy metal removal,” *Biochem. Eng. J.*, vol. 11, no. 2–3, pp. 159–166, 2002.
- [11] M. Avella, J. J. De Vlieger, M. E. Errico, S. Fischer, P. Vacca, and M. G. Volpe, “Biodegradable starch/clay nanocomposite films for food packaging applications,” *Food Chem.*, vol. 93, no. 3, pp. 467–474, 2005.
- [12] C. Elvira, J. F. Mano, J. San Roman, and R. L. Reis, “Starch-based biodegradable hydrogels with potential biomedical applications as drug delivery systems,” *Biomaterials*, vol. 23, no. 9, pp. 1955–1966, 2002.
- [13] W. K. Czaja, D. J. Young, M. Kawecki, and R. M. Brown, “The future prospects of microbial cellulose in biomedical applications,” *Biomacromolecules*, vol. 8, no. 1, pp. 1–12, 2007.



- [14] X. Qiu and S. Hu, “‘Smart’ materials based on cellulose: a review of the preparations, properties, and applications,” *Materials (Basel)*, vol. 6, no. 3, pp. 738–781, 2013.
- [15] S. R. Van Tomme and W. E. Hennink, “Biodegradable dextran hydrogels for protein delivery applications,” *Expert Rev. Med. Devices*, vol. 4, no. 2, pp. 147–164, 2007.
- [16] I. Vroman and L. Tighzert, “Biodegradable polymers,” *Materials (Basel)*, vol. 2, no. 2, pp. 307–344, 2009.
- [17] S. Li *et al.*, “Antibacterial hydrogels,” *Adv. Sci.*, vol. 5, no. 5, p. 1700527, 2018.
- [18] E. Caló and V. V Khutoryanskiy, “Biomedical applications of hydrogels: A review of patents and commercial products,” *Eur. Polym. J.*, vol. 65, pp. 252–267, 2015.
- [19] J. Maitra and V. K. Shukla, “Cross-linking in hydrogels-a review,” *Am. J. Polym. Sci*, vol. 4, no. 2, pp. 25–31, 2014.
- [20] A. Pinheiro, A. Cooley, J. Liao, R. Prabhu, and S. Elder, “Comparison of natural crosslinking agents for the stabilization of xenogenic articular cartilage,” *J. Orthop. Res.*, vol. 34, no. 6, pp. 1037–1046, 2016.
- [21] J. Zhao *et al.*, “Preparation of the polyelectrolyte complex hydrogel of

- biopolymers via a semi-dissolution acidification sol-gel transition method and its application in solid-state supercapacitors,” *J. Power Sources*, vol. 378, pp. 603–609, 2018.
- [22] W. Zhao, X. Jin, Y. Cong, Y. Liu, and J. Fu, “Degradable natural polymer hydrogels for articular cartilage tissue engineering,” *J. Chem. Technol. Biotechnol.*, vol. 88, no. 3, pp. 327–339, 2013.
- [23] E. M. Ahmed, “Hydrogel: Preparation, characterization, and applications: A review,” *J. Adv. Res.*, vol. 6, no. 2, pp. 105–121, 2015.
- [24] Z. Maolin, L. Jun, Y. Min, and H. Hongfei, “The swelling behavior of radiation prepared semi-interpenetrating polymer networks composed of polyNIPAAm and hydrophilic polymers,” *Radiat. Phys. Chem.*, vol. 58, no. 4, pp. 397–400, 2000.
- [25] V. S. Meka, M. K. G. Sing, M. R. Pichika, S. R. Nali, V. R. M. Kolapalli, and P. Kesharwani, “A comprehensive review on polyelectrolyte complexes,” *Drug Discov. Today*, vol. 22, no. 11, pp. 1697–1706, 2017.
- [26] V. B. V Maciel, C. M. P. Yoshida, and T. T. Franco, “Chitosan/pectin polyelectrolyte complex as a pH indicator,” *Carbohydr. Polym.*, vol. 132, pp. 537–545, 2015.
- [27] S. Ondaral, C. Ankerfors, L. Ödberg, and L. Wagberg, “Surface-induced rearrangement of polyelectrolyte complexes: Influence of complex

- composition on adsorbed layer properties,” *Langmuir*, vol. 26, no. 18, pp. 14606–14614, 2010.
- [28] A. V Il’Ina and V. P. Varlamov, “Chitosan-based polyelectrolyte complexes: a review,” *Appl. Biochem. Microbiol.*, vol. 41, no. 1, pp. 5–11, 2005.
- [29] S. Dakhara and C. Anajwala, “Polyelectrolyte complex: A pharmaceutical review,” *Syst. Rev. Pharm.*, vol. 1, no. 2, p. 121, 2010.
- [30] Y. Luo and Q. Wang, “Recent development of chitosan-based polyelectrolyte complexes with natural polysaccharides for drug delivery,” *Int. J. Biol. Macromol.*, vol. 64, pp. 353–367, 2014.
- [31] Y. Wen, L. Grøndahl, M. R. Gallego, L. Jorgensen, E. H. Møller, and H. M. Nielsen, “Delivery of dermatan sulfate from polyelectrolyte complex-containing alginate composite microspheres for tissue regeneration,” *Biomacromolecules*, vol. 13, no. 3, pp. 905–917, 2012.
- [32] D. Archana, L. Upadhyay, R. P. Tewari, J. Dutta, Y. B. Huang, and P. K. Dutta, “Chitosan-pectin-alginate as a novel scaffold for tissue engineering applications,” 2013.
- [33] J. Yang *et al.*, “Polyelectrolyte-fluorosurfactant complex-based meshes with superhydrophilicity and superoleophobicity for oil/water separation,” *Chem. Eng. J.*, vol. 268, pp. 245–250, 2015.

- [34] K. Chi and J. M. Catchmark, “Improved eco-friendly barrier materials based on crystalline nanocellulose/chitosan/carboxymethyl cellulose polyelectrolyte complexes,” *Food Hydrocoll.*, vol. 80, pp. 195–205, 2018.
- [35] G. Ladam, P. Schaad, J. C. Voegel, P. Schaaf, G. Decher, and F. Cuisinier, “In situ determination of the structural properties of initially deposited polyelectrolyte multilayers,” *Langmuir*, vol. 16, no. 3, pp. 1249–1255, 2000.
- [36] M. Schönhoff, “Self-assembled polyelectrolyte multilayers,” *Curr. Opin. Colloid Interface Sci.*, vol. 8, no. 1, pp. 86–95, 2003.
- [37] L. Séon, P. Lavalle, P. Schaaf, and F. Boulmedais, “Polyelectrolyte multilayers: a versatile tool for preparing antimicrobial coatings,” *Langmuir*, vol. 31, no. 47, pp. 12856–12872, 2015.
- [38] Z. Tang, Y. Wang, P. Podsiadlo, and N. A. Kotov, “Biomedical applications of layer-by-layer assembly: from biomimetics to tissue engineering,” *Adv. Mater.*, vol. 18, no. 24, pp. 3203–3224, 2006.
- [39] D. Volodkin, A. Skirtach, and H. Möhwald, “Bioapplications of light-sensitive polymer films and capsules assembled using the layer-by-layer technique,” *Polym. Int.*, vol. 61, no. 5, pp. 673–679, 2012.
- [40] K. Glinel, C. Déjugnat, M. Prevot, B. Schöler, M. Schönhoff, and R. v Klitzing, “Responsive polyelectrolyte multilayers,” *Colloids Surfaces A Physicochem. Eng. Asp.*, vol. 303, no. 1–2, pp. 3–13, 2007.

- [41] B. Tieke, F. Van Ackern, L. Krasemann, and A. Toutianoush, "Ultrathin self-assembled polyelectrolyte multilayer membranes," *Eur. Phys. J. E*, vol. 5, no. 1, pp. 29–39, 2001.
- [42] J. B. Schlenoff, S. T. Dubas, and T. Farhat, "Sprayed polyelectrolyte multilayers," *Langmuir*, vol. 16, no. 26, pp. 9968–9969, 2000.
- [43] X. Su, B.-S. Kim, S. R. Kim, P. T. Hammond, and D. J. Irvine, "Layer-by-layer-assembled multilayer films for transcutaneous drug and vaccine delivery," *ACS Nano*, vol. 3, no. 11, pp. 3719–3729, 2009.
- [44] G. Tiwari *et al.*, "Drug delivery systems: An updated review," *Int. J. Pharm. Investig.*, vol. 2, no. 1, p. 2, 2012.
- [45] R. S. Langer and N. A. Peppas, "Present and future applications of biomaterials in controlled drug delivery systems," *Biomaterials*, vol. 2, no. 4, pp. 201–214, 1981.
- [46] N. Mishra, P. Pant, A. Porwal, J. Jaiswal, and M. Aquib, "Targeted drug delivery: a review," *Am. J. Pharm. Tech. Res*, vol. 6, pp. 2249–3387, 2016.
- [47] Y. Qiu and K. Park, "Environment-sensitive hydrogels for drug delivery," *Adv. Drug Deliv. Rev.*, vol. 53, no. 3, pp. 321–339, 2001.
- [48] K. Ariga, Y. M. Lvov, K. Kawakami, Q. Ji, and J. P. Hill, "Layer-by-layer self-assembled shells for drug delivery," *Adv. Drug Deliv. Rev.*, vol. 63, no. 9,

pp. 762–771, 2011.

- [49] C. Mircioiu *et al.*, “Mathematical Modeling of Release Kinetics from Supramolecular Drug Delivery Systems,” *Pharmaceutics*, vol. 11, no. 3, p. 140, 2019.
- [50] J. Siepmann and F. Siepmann, “Modeling of diffusion controlled drug delivery,” *J. Control. release*, vol. 161, no. 2, pp. 351–362, 2012.
- [51] P. Costa and J. M. S. Lobo, “Modeling and comparison of dissolution profiles,” *Eur. J. Pharm. Sci.*, vol. 13, no. 2, pp. 123–133, 2001.
- [52] M. L. Bruschi, “Mathematical models of drug release,” *Strateg. to modify drug release from Pharm. Syst.*, vol. 63, 2015.
- [53] N. J. Percival, “Classification of wounds and their management,” *Surg.*, vol. 20, no. 5, pp. 114–117, 2002.
- [54] K. Nuutila, S. Katayama, J. Vuola, and E. Kankuri, “Human wound-healing research: issues and perspectives for studies using wide-scale analytic platforms,” *Adv. wound care*, vol. 3, no. 3, pp. 264–271, 2014.
- [55] S. al Guo and L. A. DiPietro, “Factors affecting wound healing,” *J. Dent. Res.*, vol. 89, no. 3, pp. 219–229, 2010.
- [56] K. C. Broussard and J. G. Powers, “Wound dressings: selecting the most

- appropriate type,” *Am. J. Clin. Dermatol.*, vol. 14, no. 6, pp. 449–459, 2013.
- [57] C. Valenta and B. G. Auner, “The use of polymers for dermal and transdermal delivery,” *Eur. J. Pharm. Biopharm.*, vol. 58, no. 2, pp. 279–289, 2004.
- [58] J.-S. Yang, Y.-J. Xie, and W. He, “Research progress on chemical modification of alginate: A review,” *Carbohydr. Polym.*, vol. 84, no. 1, pp. 33–39, 2011.
- [59] S. N. Pawar and K. J. Edgar, “Alginate derivatization: a review of chemistry, properties and applications,” *Biomaterials*, vol. 33, no. 11, pp. 3279–3305, 2012.
- [60] J. Venkatesan, I. Bhatnagar, P. Manivasagan, K.-H. Kang, and S.-K. Kim, “Alginate composites for bone tissue engineering: a review,” *Int. J. Biol. Macromol.*, vol. 72, pp. 269–281, 2015.
- [61] C. K. Yeom and K.-H. Lee, “Characterization of sodium alginate membrane crosslinked with glutaraldehyde in pervaporation separation,” *J. Appl. Polym. Sci.*, vol. 67, no. 2, pp. 209–219, 1998.
- [62] M. George and T. E. Abraham, “Polyionic hydrocolloids for the intestinal delivery of protein drugs: alginate and chitosan—a review,” *J. Control. release*, vol. 114, no. 1, pp. 1–14, 2006.
- [63] A. Wassermann, “Alginic acid-acetate,” *Nature*, vol. 158, no. 4008, p. 271,

1946.

- [64] R. J. Coleman, G. Lawrie, L. K. Lambert, M. Whittaker, K. S. Jack, and L. Grøndahl, "Phosphorylation of alginate: synthesis, characterization, and evaluation of in vitro mineralization capacity," *Biomacromolecules*, vol. 12, no. 4, pp. 889–897, 2011.
- [65] S. B. Shah, C. P. Patel, and H. C. Trivedi, "Ceric-induced grafting of acrylate monomers onto sodium alginate," *Carbohydr. Polym.*, vol. 26, no. 1, pp. 61–67, 1995.
- [66] H. Ronghua, D. Yumin, and Y. Jianhong, "Preparation and in vitro anticoagulant activities of alginate sulfate and its quaterized derivatives," *Carbohydr. Polym.*, vol. 52, no. 1, pp. 19–24, 2003.
- [67] M.-C. Carre, C. Delestre, P. Hubert, and E. Dellacherie, "Covalent coupling of a short polyether on sodium alginate: synthesis and characterization of the resulting amphiphilic derivative," *Carbohydr. Polym.*, vol. 16, no. 4, pp. 367–379, 1991.
- [68] A. Dalmoro, A. A. Barba, G. Lamberti, M. Grassi, and M. d'Amore, "Pharmaceutical applications of biocompatible polymer blends containing sodium alginate," *Adv. Polym. Technol.*, vol. 31, no. 3, pp. 219–230, 2012.
- [69] W.-R. Lee *et al.*, "The biological effects of topical alginate treatment in an animal model of skin wound healing," *Wound repair Regen.*, vol. 17, no. 4,



pp. 505–510, 2009.

- [70] A. I. Attwood, “Calcium alginate dressing accelerates split skin graft donor site healing,” *Br. J. Plast. Surg.*, vol. 42, no. 4, pp. 373–379, 1989.
- [71] D.-H. Roh *et al.*, “Wound healing effect of silk fibroin/alginate-blended sponge in full thickness skin defect of rat,” *J. Mater. Sci. Mater. Med.*, vol. 17, no. 6, pp. 547–552, 2006.
- [72] K. Murakami *et al.*, “Hydrogel blends of chitin/chitosan, fucoidan and alginate as healing-impaired wound dressings,” *Biomaterials*, vol. 31, no. 1, pp. 83–90, 2010.
- [73] L. Cao, Y. Hu, L. Zhang, C. Ma, X. Wang, and J. Wang, “Synthesis of cross-linked poly (4-vinylpyridine) and its copolymer microgels using supercritical carbon dioxide: Application in the adsorption of copper (II),” *J. Supercrit. Fluids*, vol. 58, no. 2, pp. 233–238, 2011.
- [74] R. M. Fuoss and U. P. Strauss, “Polyelectrolytes. II. Poly-4-vinylpyridonium chloride and poly-4-vinyl-N-n-butylpyridonium bromide,” *J. Polym. Sci.*, vol. 3, no. 2, pp. 246–263, 1948.
- [75] R. Bryaskova, S. Vircheva, S. Miloshev, N. Dishovsky, and R. Tzoneva, “Design and synthesis of gold-loaded micelles based on poly (ethylene glycol) and poly (4-vinyl pyridine) triblock copolymers for biomedical applications,” *Colloid Polym. Sci.*, vol. 295, no. 3, pp. 487–494, 2017.

- [76] N. Sahiner and O. Ozay, “Responsive tunable colloidal soft materials based on p (4-VP) for potential biomedical and environmental applications,” *Colloids Surfaces A Physicochem. Eng. Asp.*, vol. 378, no. 1–3, pp. 50–59, 2011.
- [77] C. P. Dhanalakshmi, L. Vijayalakshmi, and V. Narayanan, “Nanocomposites of Carbonated Hydroxyapatite/Poly (4-vinyl pyridine-co-styrene): Synthesis, Characterization and its Application,” in *Nano Hybrids*, 2012, vol. 2, pp. 65–85.
- [78] J. M. J. Fréchet and M. V. de Meftahi, “Poly (vinyl pyridine) s: Simple reactive polymers with multiple applications,” *Br. Polym. J.*, vol. 16, no. 4, pp. 193–198, 1984.
- [79] J. U. N. Fang, Z. Gu, D. Gang, C. Liu, E. S. Ilton, and B. Deng, “Cr (VI) removal from aqueous solution by activated carbon coated with quaternized poly (4-vinylpyridine),” *Environ. Sci. Technol.*, vol. 41, no. 13, pp. 4748–4753, 2007.
- [80] H. B. Sonmez and N. Bicak, “Quaternization of poly (4-vinyl pyridine) beads with 2-chloroacetamide for selective mercury extraction,” *React. Funct. Polym.*, vol. 51, no. 1, pp. 55–60, 2002.
- [81] \.I Alper \.I\cso\uglu, C. Demirkan, M. G. \cSeker, K. Tuzlako\uglu, and S. D. \.I\cso\uglu, “Antibacterial Bilayered Skin Patches Made of HPMA and Quaternary Poly (4-vinyl pyridine),” *Fibers Polym.*, vol. 19, no. 11, pp. 2229–2236, 2018.

- [82] D. E. Tallman and G. G. Wallace, "Preparation and preliminary characterization of a poly (4-vinylpyridine) complex of a water-soluble polyaniline," *Synth. Met.*, vol. 90, no. 1, pp. 13–18, 1997.
- [83] G. K. Such, A. P. R. Johnston, and F. Caruso, "Engineered hydrogen-bonded polymer multilayers: from assembly to biomedical applications," *Chem. Soc. Rev.*, vol. 40, no. 1, pp. 19–29, 2010.
- [84] T. R. Farhat and J. B. Schlenoff, "Corrosion control using polyelectrolyte multilayers," *Electrochem. solid-state Lett.*, vol. 5, no. 4, pp. B13--B15, 2002.
- [85] M. I. Tadros, "Controlled-release effervescent floating matrix tablets of ciprofloxacin hydrochloride: Development, optimization and in vitro--in vivo evaluation in healthy human volunteers," *Eur. J. Pharm. Biopharm.*, vol. 74, no. 2, pp. 332–339, 2010.
- [86] M. E. Olivera *et al.*, "Biowaiver monographs for immediate release solid oral dosage forms: Ciprofloxacin hydrochloride," *J. Pharm. Sci.*, vol. 100, no. 1, pp. 22–33, 2011.
- [87] M. C. Garcia *et al.*, "A novel gel based on an ionic complex from a dendronized polymer and ciprofloxacin: Evaluation of its use for controlled topical drug release," *Mater. Sci. Eng. C*, vol. 69, pp. 236–246, 2016.
- [88] Z. Orhan *et al.*, "The preparation of ciprofloxacin hydrochloride-loaded chitosan and pectin microspheres: their evaluation in an animal osteomyelitis

- model,” *J. Bone Joint Surg. Br.*, vol. 88, no. 2, pp. 270–275, 2006.
- [89] R. S. Al-Kassas and M. M. El-Khatib, “Ophthalmic controlled release in situ gelling systems for ciprofloxacin based on polymeric carriers,” *Drug Deliv.*, vol. 16, no. 3, pp. 145–152, 2009.
- [90] P. R. Sarika and N. R. James, “Polyelectrolyte complex nanoparticles from cationised gelatin and sodium alginate for curcumin delivery,” *Carbohydr. Polym.*, vol. 148, pp. 354–361, 2016.
- [91] E.-S. I. El-Shafey, H. Al-Lawati, and A. S. Al-Sumri, “Ciprofloxacin adsorption from aqueous solution onto chemically prepared carbon from date palm leaflets,” *J. Environ. Sci.*, vol. 24, no. 9, pp. 1579–1586, 2012.
- [92] M. Alokour and E. Yilmaz, “Photoinitiated synthesis of poly (poly (ethylene glycol) methacrylate-co-diethyl amino ethyl methacrylate) superabsorbent hydrogels for dye adsorption,” *J. Appl. Polym. Sci.*, vol. 136, no. 26, p. 47707, 2019.
- [93] M. Abdollahi, M. Alboofetileh, R. Behrooz, M. Rezaei, and R. Miraki, “Reducing water sensitivity of alginate bio-nanocomposite film using cellulose nanoparticles,” *Int. J. Biol. Macromol.*, vol. 54, pp. 166–173, 2013.
- [94] L. C. Cesteros, J. R. Isasi, and I. Katime, “Hydrogen bonding in poly (4-vinylpyridine)/poly (vinyl acetate-co-vinyl alcohol) blends. An infrared study,” *Macromolecules*, vol. 26, no. 26, pp. 7256–7262, 1993.

- [95] V. P. Panov, L. A. Kazarin, V. I. Dubrovin, V. V Gusev, and Y. É. Kirsh, "Infrared spectra of atactic poly-4-vinylpyridine," *J. Appl. Spectrosc.*, vol. 21, no. 5, pp. 1504–1510, 1974.
- [96] Z. Tong *et al.*, "Preparation, characterization and properties of alginate/poly ( $\gamma$ -glutamic acid) composite microparticles," *Mar. Drugs*, vol. 15, no. 4, p. 91, 2017.
- [97] Z. Wang, S. Hu, and H. Wang, "Scale-Up Preparation and Characterization of Collagen/Sodium Alginate Blend Films," *J. Food Qual.*, vol. 2017, 2017.
- [98] B. Zahiri, P. K. Sow, C. H. Kung, and W. Mérida, "Understanding the wettability of rough surfaces using simultaneous optical and electrochemical analysis of sessile droplets," *J. Colloid Interface Sci.*, vol. 501, pp. 34–44, 2017.
- [99] A. Gulzar, S. Gai, P. Yang, C. Li, M. B. Ansari, and J. Lin, "Stimuli responsive drug delivery application of polymer and silica in biomedicine," *J. Mater. Chem. B*, vol. 3, no. 44, pp. 8599–8622, 2015.
- [100] H. Dias Murbach *et al.*, "Ciprofloxacin release using natural rubber latex membranes as carrier," *Int. J. Biomater.*, vol. 2014, 2014.
- [101] M. A. Kalam *et al.*, "Release kinetics of modified pharmaceutical dosage forms: a review," *Cont J Pharm Sci*, vol. 1, pp. 30–35, 2007.

[102] J. Siepmann and N. A. Peppas, “Higuchi equation: derivation, applications, use and misuse,” *Int. J. Pharm.*, vol. 418, no. 1, pp. 6–12, 2011.